

NOTICE: This is the author's version of a work that was accepted for publication in Precambrian Research. Changes resulting from the publishing process, such as peer review, editing, corrections, structural formatting, and other quality control mechanisms may not be reflected in this document. Changes may have been made to this work since it was submitted for publication. A definitive version was subsequently published in Precambrian Research, Vol. 244, (2013). doi: 10.1016/j.precamres.2013.05.014

Mesoproterozoic paleogeography: supercontinent and beyond

Sergei A. Pisarevsky^{a,b}, Sten-Åke Elming^c, Lauri J. Pesonen^d, Zheng-Xiang Li^a

^a Australian Research Council Centre of Excellence for Core to Crust Fluid Systems (CCFS) and the Institute for Geoscience Research (TIGeR), Department of Applied Geology, Curtin University, GPO Box U1987, Perth, WA 6845, Australia.

^b School of Earth and Environment, University of Western Australia, 35 Stirling Highway, Crawley, WA 6009, Australia

^c Department of Civil, Environmental and Natural resources engineering, Luleå University of Technology, SE-07187 Luleå, Sweden.

^d Division of Geophysics and Astronomy, Department of Physics, University of Helsinki, PO Box 64 (Gustaf Hällströmin katu 2), FIN-00014 Helsinki, Finland.

Abstract

A set of global paleogeographic reconstructions for the 1770–1270 Ma time interval is presented here through a compilation of reliable paleomagnetic data (at the 2009 Nordic Paleomagnetic Workshop in Luleå, Sweden) and geological constraints. Although currently available paleomagnetic results do not rule out the possibility of the formation of a supercontinent as early as ca. 1750 Ma, our synthesis suggests that the supercontinent Nuna/Columbia was assembled by at least ca. 1650–1580 Ma through joining at least two stable continental landmasses formed by ca. 1.7 Ga: West Nuna (Laurentia, Baltica and possibly India) and East Nuna (North, West and South Australia, Mawson craton of Antarctica and North China). It is possible, but not convincingly proven, that Siberia and Congo/São Francisco were combined as a third rigid continental entity and collided with Nuna at ca. 1500 Ma. Nuna is suggested to have broken up at ca. 1450–1380 Ma. West Nuna, Siberia and possibly Congo/São Francisco were rigidly connected until after 1270 Ma. East Nuna was deformed during the breakup, and North China separated from it. There is currently no strong evidence indicating that Amazonia, West Africa and Kalahari were parts of Nuna.

29 *Key words:* Mesoproterozoic, global, paleogeography, supercontinent, paleomagnetism.

30 **1. Introduction**

31 There has been a growing interest in the hypothesised pre-Rodinian supercontinent,
32 variously called Nuna, Columbia, or Hudsonland (e.g., Hoffman, 1997; Meert, 2002; Pesonen
33 et al., 2003; Zhao et al., 2002, 2004). One of the main geological arguments used for this
34 hypothesis is in the presence of 2.1–1.8 Ga orogens in a majority of continents (e.g., Zhao et
35 al., 2004), and it was suggested that some or all of these orogens resulted from the assembly
36 of this supercontinent. However, most reconstructions are highly speculative in nature,
37 mainly due to the lack of adequate high quality paleomagnetic data to provide independent
38 constraints.

39 At the 2009 Nordic Paleomagnetic Workshop in Luleå (Sweden; Elming and Pesonen,
40 2010), it was concluded that there are about one hundred late Paleoproterozoic to
41 Mesoproterozoic paleopoles (most of them are from Laurentia, Baltica, Siberia and Australia)
42 of ‘reasonable’ quality and they can be used for late Paleo- to Mesoproterozoic
43 reconstructions. In this study we slightly updated the Luleå data compilation utilising more
44 recently published paleomagnetic and geochronological results (Table 1). Most of the
45 paleopoles in Table 1 are considered to be of high quality, but we have also included some
46 less reliable poles (shown in italics), which were used only as a “second-order” constraints
47 for paleogeographic reconstructions. In most cases these less reliable poles are either poorly
48 dated or have not averaged out secular variation of geomagnetic field and are therefore
49 marked as Virtual Geomagnetic Poles (VGPs). Hereafter we shall call them ‘non-key’ poles.
50 In the following sections we use (directly and indirectly) about a hundred ca. 1800–1000 Ma
51 poles in an attempt to reconstruct the global distribution of continents and the history of their
52 drift in the late Paleoproterozoic and much of the Mesoproterozoic (mainly the 1770–1270
53 Ma time interval). The paleogeography of the 1270–1000 Ma time period is enigmatic and

54 has to be analysed separately and published elsewhere. However, we consider few elements
55 of this late Mesoproterozoic paleogeography to provide some clues for understanding of older
56 events.

57 The paleomagnetic data presented in Table 1 and Figure 1 clearly demonstrate that both
58 temporal and spatial distributions of the 1800–1000 Ma data are very uneven. Even from the
59 paleomagnetically most thoroughly studied Laurentia there are still not enough data for the
60 construction of a reliable Apparent Polar Wander Path (APWP) for the entire period.

61 Paleomagnetic databases for other continents are even less complete, and paleopositions of
62 some continents (e.g. South China, Rio de La Plata, São Francisco, West Africa) are not
63 paleomagnetically constrained at all.

64 Comparison of lengths and shapes of APWPs is a normal technique for testing
65 supercontinent hypotheses – as long as two continents have travelled together as parts of a
66 single plate, they should have identical APWPs. In the absence of well defined APWPs, as
67 the first approximation, we can use pairs of coeval paleomagnetic poles from two cratonic
68 blocks for a test. If the distance between two paleopoles with ages X and Y of one continent
69 is the same as the distance between two paleopoles with ages X and Y of another continent,
70 we can suggest that these continents could have been parts of the same supercontinent
71 between times X and Y (e.g. Evans and Pisarevsky, 2009), provided that the Geocentric Axial
72 Dipole (GAD) model is valid for Precambrian (Veikkolainen et al., 2012). This is a
73 necessary, but not sufficient condition. If there are more than two such coeval and equidistant
74 pairs of poles, the probability of rigid co-travelling increases. Even in this case the
75 paleomagnetic reconstruction of mutual positions of two continents must still be tested by
76 geological data. In addition, we can use single poles to constrain the paleolatitudes of a given
77 continent, and examine the possibility of it being a part of a supercontinent by comparing
78 both their paleolatitudes and geological linkages. In the following section we mainly use the

79 methods of comparing the APWPs or paired paleopoles between two continents to examine
80 their potential links during the late Paleo- to Mesoproterozoic.

81 **2. Baltica and eastern Laurentia**

82 Paleomagnetic data for the period 1800–1270 Ma are most abundant for Laurentia and
83 Baltica (Table 1, Fig.1). Salminen and Pesonen (2007) demonstrated that paleomagnetic data
84 support the existence of a single Baltica–Laurentia continent from ca. 1760 Ma until ca. 1270
85 Ma. Their reconstruction was similar, but not identical, to the reconstruction of Gower et al.
86 (1990), which was built by matching pre-Neoproterozoic crustal blocks and orogenic belts of
87 these cratons. The difference between the “geological” reconstruction of Gower et al. (1990)
88 and the “paleomagnetic” reconstruction of Salminen and Pesonen (2007) is within the
89 precision limits of both paleomagnetic and geochronological methods. A similar
90 paleomagnetically-based reconstruction was given by Wu et al. (2005).

91 Baltica was assembled sometime during 1800–1700 Ma (Bogdanova et al., 2008; Elming et
92 al., 2010) by the collision between Sarmatia/Volgo-Uralia and Fennoscandia along the
93 Central Russian collision belt (Fig. 2). Pisarevsky and Bylund (2010) slightly modified the
94 Baltica-Laurentia reconstruction using new paleomagnetic data and proposed that the “best
95 fit” Laurentia- Fennoscandia reconstruction between 1790–1770 Ma and 1270–1260 Ma
96 requires an anticlockwise rotation of Fennoscandia (and the whole of Baltica after 1700 Ma)
97 to Laurentia (Fig. 2). We followed this suggestion in our reconstructions and treat Laurentia
98 and Fennoscandia (Baltica after 1700 Ma) as a single continent until 1270 Ma.

99 The Mesoproterozoic tectonic history of Baltica is characterised by prolonged accretion
100 from the present-day west (e.g., Gorbatshev and Bogdanova, 1993; Bogdanova et al., 2001;
101 Åhäll and Connelly, 2008; Bingen et al, 2008; Bogdanova et al., 2008). The 1900–1850 Ma
102 Svecofennian orogeny culminated in the formation of the 1850–1650 Ma Transscandinavian
103 Igneous Belt (TIB), which was followed by the 1640–1520 Ma Gothian orogeny, the 1520–

104 1480 Ma Telemarkian accretionary events, the 1470–1420 Ma Hallandian-Danopolonian
105 orogeny, and eventually by the 1140–970 Ma Sveconorwegian orogeny (Bingen et al., 2008).
106 The SE margin of Laurentia has a similar history with the 1800–1700 Ma Yavapai, 1700–
107 1600 Ma Mazatzal and 1300–900 Ma Grenville orogenies (e.g., Karlstrom et al., 2001).

108 The exact timing of the post-1270 Ma breakup of Baltica from Laurentia is unclear. Park
109 (1992) suggested that it was related to the 1270 Ma giant McKenzie magmatic event and
110 Elming and Mattsson (2001) suggested that the coeval Central Scandinavian Dolerite
111 complex was a result of such a breakup. Starmer (1996) provided some structural evidence
112 that separation started at ca. 1240 Ma. Ca. 1270 Ma Laurentian and Baltican paleopoles
113 support the integrity at that time. The next oldest non-key Salla Dyke pole from Baltica and
114 the Abitibi and Nipigon poles from Laurentia (Table 1, entries 73 and 77, respectively),
115 however, indicate a wide separation between the two continents at ca. 1120 Ma.

116 **3. Siberia and northern Laurentia**

117 Based on 1050–950 Ma Laurentian and Siberian paleomagnetic data (Table 1, entries 78–
118 89) Pisarevsky and Natapov (2003) suggested that these two continents could have moved
119 coherently during that time if Siberia was located NW of Laurentia and with a significant
120 ‘gap’ between them that was presumably occupied by some yet unknown piece(s) of
121 continental crust. Wingate et al. (2009) reported a new ca 1475 Ma Siberian paleomagnetic
122 pole. This pole, together with a coeval Laurentian pole by Meert and Stuckey (2002),
123 suggests that this distant but fixed position of Siberia relative to Laurentia may be valid
124 between ca. 1500 and 1000 Ma. Such a distant relationship might explain the apparent
125 absence of any traces of the giant 1267 Ma Mackenzie igneous event in Siberia (Gladkochub
126 et al., 2006; Pisarevsky et al., 2008). Notably, these hypotheses assume that the Siberian
127 craton behaved as a rigid coherent continent since the Mesoproterozoic. However, Gurevich
128 (1984) analysed early Paleozoic Siberian paleomagnetic data and suggested that there was a

129 significant (ca. 20°) clockwise rotation of SW Siberia (the Aldan block) with respect to NW
130 Siberia (the Anabar-Angara block) during the opening of the v-shaped Vilyui syncline in
131 Devonian time. Pavlov et al. (2008) provided more geophysical, geological and
132 paleomagnetic evidence for such a rotation and reported the best estimate of Euler rotation
133 parameters (Aldan is rotated to Angara-Anabar) to be +23° about a pole at 62°N, 117°E.
134 Using these parameters, we modified the shape of pre-Devonian Siberia. This restoration also
135 caused the rotation of the ca. 1050–950 Ma Siberian poles (Pavlov et al., 2000, 2002; Gallet
136 et al., 2000; Table 1, entries 84–89) from the Aldan block (Table 1). These readjustments
137 provide a tighter fit of the ca. 1500–950 Ma coeval Siberian and Laurentian poles but still
138 require a distant position of Siberia with respect to Laurentia (Fig. 3). Following this
139 paleomagnetic argument we suggest that between ca. 1500–1270 Ma Laurentia, Baltica and
140 Siberia were in a fixed position with respect to each other, implying that there might have
141 been a supercontinent during that time. Didenko et al. (2013) published two 1730–1720 Ma
142 paleopoles from the Aldan block (Table 1, entries 24–25). These poles suggest an equatorial
143 position for Siberia at 1730–1720 Ma, which is supported by three ca. 1750–1730 Ma non-
144 key Siberian poles (Table 1, entries 21–23). The best fit of these poles with the Laurentian
145 1740 Ma Cleaver Dykes pole (Table 1, entry 20) suggests a larger distance between the two
146 continents than shown in Fig. 3. We conclude that Siberia had not joined the Laurentia-
147 Baltica system by 1740–1720 Ma.

148 **4. Australia and western Laurentia**

149 1800–1500 Ma Australian paleopoles are relatively abundant (Table 1; Fig. 1), and most
150 are from Northern Australia. There is a general agreement that Australia was assembled by
151 collision of three Archean to Paleoproterozoic building blocks – the North Australian, West
152 Australian and South Australian cratons (NAC, WAC and SAC). However, the timing of this
153 assembly is still debated (e.g. Myers et al., 1996; Betts and Giles, 2006; Schmidt et al., 2006;

154 Cawood and Korsch, 2008; Li and Evans, 2011). In this study we accept the model of Li and
155 Evans (2011), suggesting the proximity between these three elements since ca. 1800 Ma, but
156 in a configuration different from the present-day one until ca. 650 Ma. There was an
157 intraplate rotation between WAC–SAC and NAC during 650–550 Ma which resulted in the
158 present-day configuration. We also adapted the hypothesis of a clockwise rotation of the
159 SAC at ca. 1500–1300 Ma that resulted in a collision with the WAC during the Albany-
160 Fraser orogeny (Betts and Giles, 2006). It has been suggested that the Gawler craton of the
161 SAC has a continuation into the Mawson Craton in Antarctica (e.g. Fanning et al., 1995;
162 Fitzsimons, 2003; Boger, 2011 and references therein), but the size and shape of the Mawson
163 craton is yet unclear. In our reconstructions we follow this suggestion and use the shape of
164 the Mawson craton as it was shown by Powell and Pisarevsky (2002).

165 Precambrian connections between western Laurentia and Australia (SWEAT, AUSWUS,
166 AUSMEX, “Missing Link”) have been debated for over two decades (e.g. Moores, 1991;
167 Dalziel, 1991; Brookfield, 1993; Li et al., 1995; Karlstrom et al., 2001; Burrett and Berry,
168 2000; Wingate et al. 2002). A detailed review of Neoproterozoic (after 1000 Ma) Australia-
169 Laurentia fits was presented by Li et al. (2008a). However, Pisarevsky et al. (2003a)
170 demonstrated that neither of those reconstructions is valid for Mesoproterozoic time (ca. 1200
171 Ma) according to paleomagnetic data. Analysing 1800–1580 Ma geological and
172 paleomagnetic data from North Australia, Betts et al. (2008, 2009) showed the possibility of a
173 “SWEAT-like” reconstruction with North Australia located close to the north-western tip of
174 Laurentia. With new paleomagnetic analyses Zhang et al. (2012) supported this idea of North
175 Australia being fixed to NW Laurentia in such a SWEAT-like configuration. Here we modify
176 this model, suggesting that though the two continents were in a geographical proximity, their
177 final assembly occurred at 1650–1600 Ma during the Racklan orogeny (Fig. 2; Furlanetto et
178 al., 2013). The reasons for such an interpretation are as follows.

179 The thick sedimentary Wernicke Supergroup was deposited in the Yukon Territory on the
180 northern part of the western Laurentian margin. The measurable thickness of this succession
181 is ca. 13 km, but the lower contact with the basement is not exposed, so the real thickness can
182 even be larger (Furlanetto et al., 2013). Seismic profile suggest the whole thickness to be up
183 to 20 km with gradually increase to the west (Mitchelmore and Cook, 1994), which is
184 characteristic of a passive continental margin, but also possible for an intracontinental basin.
185 Thorkelson et al. (2005) suggested that the two hypotheses are equally viable, noting,
186 however, that the intensity of the following ca. 1650–1600 Ma Racklan orogeny is more
187 consistent with collisional tectonics along a continental margin than intracratonic
188 deformation. If we accept the passive margin model, the initial rifting event should have
189 occurred after the end of the ca. 1900 Ma Wopmay orogeny (Hildebrand et al., 2010). Cook
190 and Erdmer (2005) suggested that the initiation of the Wernicke Basin formation occurred
191 between 1840–1760 Ma. Thorkelson et al. (2005) suggested that the minimum age of
192 Wernicke sedimentation is constrained by the 1720 Ma Bonnet Plume River intrusions,
193 which apparently cut the Wernicke sediments. However, Furlanetto et al. (2013) challenged
194 this cross-cutting relationship after finding ca. 1640 Ma detrital zircons in the lower part of
195 the Wernicke Supergroup. These authors suggest that the Bonnet Plume River intrusions
196 originated in an offshore volcanic arc terrane (Bonnetia) that was accreted to Laurentia
197 during the ca. 1600 Ma second stage of the Racklan orogeny. If true, this model is supportive
198 of the hypothesis of a late Paleoproterozoic oceanic margin in this part of western Laurentia,
199 since it is hard to imagine a volcanic arc in an intracontinental basin. The timing of initiation
200 of Wernicke sedimentation is still unclear, since the lowermost part of the supergroup is not
201 exposed, but we assume that, at 1770 Ma, there was an oceanic space west of western
202 Laurentia. To the south of the Mackenzie Mts the Muskwa assemblage is a 6 km thick
203 sequence of essentially unmetamorphosed, predominantly fine-grained siliciclastic and

204 carbonate strata with a maximum age of 1766 Ma (youngest detrital zircon) (Ross et al.,
205 2001). Seismic studies show a passive margin fabric (Cook et al., 2004).

206 There has been a rapidly improved understanding of the Late Paleoproterozoic and
207 Mesoproterozoic tectonic evolution of eastern North Australia in the last decade (e.g. Giles et
208 al., 2002; Betts and Giles, 2006; Fraser et al., 2007; Gibson et al., 2008; Betts et al., 2008,
209 2009). These studies led to somewhat contrasting tectonic models. Detailed descriptions of
210 these models are beyond the scope of our study. However, there are several common
211 elements in these models relevant to the Australia-Laurentia reconstructions between
212 ca.1800–1600 Ma. In particular, sedimentation in the eastern basins of North Australia is
213 suggested to have persisted until ca. 1600–1550 Ma, when sedimentation ended, which may
214 be related to the westward vergence of the Jana orogeny in the Georgetown, Coen, Yambo,
215 and Dargalong inliers (Betts and Giles, 2006 and references therein). This is roughly
216 reminiscent of the development of the Wernicke Supergroup and to the Racklan orogeny. The
217 tectonic history of the eastern edge of the North Australian craton between ca. 1800–1550 Ma
218 includes several changes of the tectonic regime, which are, in our view, not consistent with a
219 purely intracontinental environment, implied by rigid connection with Laurentia. A
220 geochemical study of the 1685–1640 Ma mafic rocks in the Georgetown Inlier (Baker et al.,
221 2010) led the authors to suggest that these volcanic rocks were associated with a volcanic
222 passive margin. Betts and Giles (2006) suggested a mid-oceanic ridge east of North Australia
223 at 1650–1620 Ma and convergence with western Laurentia at 1610–1570 Ma. All this implies
224 that North Australia faced an ocean (maybe a small remnant sea like the Mediterranean) in the
225 present east at ca. 1800–1550 Ma. It is difficult to estimate the width of this ocean. At some
226 stages it may have been a Mediterranean-type basin (this may explain the variety of tectonic
227 styles within it), which explains a paleomagnetically permitted proximity of North Australia
228 and Laurentia at ca. 1800–1600 Ma. However, it is very unlikely that these continents were at

229 exactly the same mutual position as shown in the 1780–1650 Ma reconstructions of Betts et
230 al. (2008). We propose a series of 1770–1580 Ma paleomagnetically supported
231 reconstructions in which Australian and Antarctic continental blocks approached NW
232 Laurentia from relatively distal positions until assembly at ca. 1600–1550 Ma (Figs.7–10).

233 Pisarevsky et al. (2003a) demonstrated that Australia and Laurentia were widely separated
234 at ca. 1200 Ma, which means that there was a breakup sometime after 1550 Ma. It is difficult
235 to establish a precise time for this breakup because there are no reliable 1500–1220 Ma
236 paleomagnetic data for Australia. Betts and Giles (2006) loosely constrained this rifting to
237 between 1500–1330 Ma. This breakup can be related to the opening of the Belt-Purcell basin
238 in western Laurentia, constrained by the 1469–1457 Ma Moyie sills intruded into still-wet
239 sediments of the lowermost Prichard Formation of the Belt Supergroup (Elston et al., 2002
240 and references therein). Goodge et al. (2008) reported a 1441 ± 6 Ma granitoid clast found in
241 the central part of the Transantarctic Mountains with Hf and Nd isotopic compositions similar
242 to the ca. 1500–1300 Ga Laurentian granites. The authors suggested that this supports a
243 Laurentia-East Antarctica (Mawson craton) connection at ca. 1440 Ma. If so, the separation
244 between Australia-Mawson and Laurentia could not have begun before that. In the northern
245 part of western Laurentia the breakup could have been associated with the rift-related 1.38 Ga
246 Hart River magmatism, followed by deposition of the Pinguicula Group (Medig et al., 2010).

247 **5. North China and Australia**

248 The 1780–1760 Ma and 1460–1410 Ma paleopoles from North China (Table 1, entries 11–
249 12 and 53) permit a fixed position of this continent juxtaposed to Australia (Figs.7–13) as
250 was proposed by Zhang et al (2012). We suggest a similar North China-Australia fit. The
251 1780–1750 Ma andesite-dominated Xiong'er Group at the southern margin of the North
252 China Craton has been suggested to represent an Andean-type continental margin (e.g., Zhao,
253 2009; He et al., 2010; Zhao and Cawood, 2012). The position of North China after the

254 suggested breakup of Australia and Laurentia is constrained by a new ca. 1350 Ma pole of
255 Chen et al. (2013; Table 1, entry 61).

256 **6. Amazonia and West Africa**

257 Amazonia has two coeval pairs of poles at ca. 1790 Ma and at ca. 1420 Ma (Table 1,
258 entries 14–15, 54–55; Fig. 1). In this study we discuss the SAMBA-type and other
259 reconstructions of this continent (Johansson, 2009; Bispo-Santos et al., 2008; Elming et al.,
260 2009a; Zhang et al., 2012). We also follow the generally accepted hypothesis of Trompette
261 (1994) that West Africa and Amazonia constituted a rigid continent since the
262 Mesoproterozoic, similar to their Gondwanan configuration.

263 The original SAMBA reconstruction (Johansson, 2009) is based on the similar late
264 Paleoproterozoic–Mesoproterozoic accretionary history of Amazonia and Baltica. In
265 particular, it was suggested that the 1900–1850 Ma Svecofennian orogen in Baltica continues
266 into the 1980–1810 Ma Ventuari-Tapajós province in Amazonia, and that the 1850–1650 Ma
267 TIB and the 1640–1520 Ma Gothian orogen have their continuation into the 1780–1550 Ma
268 Rio Negro–Juruena province (Fig.4). In the SAMBA model the combined Baltica–Amazonia–
269 West Africa continent existed as a rigid body from 1800 Ma until after 900 Ma (Johansson,
270 2009). Fuck et al. (2008), however, argued that the Ventuari-Tapajós and Rio Negro-Juruena
271 provinces are truncated by the younger Grenville-age orogen in their northern parts (Fig.4),
272 which questions the continuity of Baltican and Amazonian accretionary belts.

273 Bispo-Santos et al. (2008) argued that their 1789 ± 7 Ma Colider Volcanics paleopole
274 (Table 1, entry 14) requires some distance between Amazonia and Baltica at ca. 1790 Ma. In
275 their reconstruction North China is located between these two continents. D’Agrella-Filho et
276 al. (2012) and Bispo-Santos et al. (2012) published two coeval, closely located and well-
277 dated ca. 1420 Ma Indiavaí and Nova Guarita poles (Table 1, entries 54–55). D’Agrello-Filho
278 et al. (2012) demonstrated that these poles do not support the SAMBA reconstruction at ca.

279 1420 Ma. Recently Reis et al. (in press) cited a new 1790 Ma pole for the Avanavero
280 intrusion, for which the primary origin of the magnetization is supported by a contact test
281 (Table 1, entry 15). This pole is coeval to the Colider pole, but the angular difference
282 between them is about 48°. Unfortunately, no details of this paleomagnetic study have been
283 provided. Reis et al. (in press) argue that the Avanavero pole supports the SAMBA
284 reconstruction at ca. 1790 Ma, but the authors admit that this requires the integrity of Baltica
285 by 1790 Ma. Meanwhile, Baltica was not yet assembled at that time, and Sarmatia/Volgo-
286 Uralia was separated from Fennoscandia (e.g. Bogdanova et al., 2008; Elming et al., 2010).
287 Reis et al. (in press) give two alternative explanations for the significant angular difference
288 between coeval Avanavero and Collider poles. The first explanation is that the Avanavero
289 pole is primary, but the Colider pole represents a younger remagnetisation. This explanation
290 has some merit, since the Colider pole is not supported by field tests. The second explanation
291 suggests that northern Amazonia (where the Avanavero intrusions are located) was separated
292 from southern Amazonia (location of the Colider, Indiavaí and Nova Guarita sampling areas)
293 at ca. 1790 Ma. Reis et al. (in press) suggest that these two parts of Amazonia were
294 assembled sometime after 1790 Ma.

295 In Fig.5 we show a paleomagnetic test of the SAMBA reconstruction at 1790 Ma (Fig. 5a–
296 c) and at 1420 Ma (Fig. 5d–f). Figs. 5a and 5d consider the integrity of the Amazonian
297 Craton. In the SAMBA-type configuration Amazonia is juxtaposed against Sarmatia. In this
298 scenario the Avanavero pole is close to Laurentian, Fennoscandian and Sarmatian poles of
299 similar age (Fig.5a; pole numbers are as in Table 1), which makes the SAMBA
300 reconstruction paleomagnetically permitted at ca. 1790 Ma (with some reservations about the
301 quality of the Avanavero pole), but the Colider pole does not support this reconstruction.
302 Therefore, if the SAMBA model is correct, we suggest that the Colider pole is not primary.
303 At 1420 Ma (Fig. 5d), however, both Indiavaí and Nova Guarita poles are >45° away from

304 roughly coeval Laurentian and Baltican poles, indicating that the SAMBA reconstruction is
305 not paleomagnetically permissible at 1420 Ma.

306 In Figures 5b and 5e the hypothesised displacement between southern and northern
307 Amazonia is illustrated, with the Euler pole of rotation as in Reis et al. (in press). In this
308 scenario the Avanavero and Colider poles match exactly, but the displacement is significant
309 and probably contradicts one of the key arguments for the SAMBA model – it disrupts the
310 linearity of the Ventuari-Tapajós province. At 1420 Ma the displacement makes little
311 difference compared to the first scenario (Fig.5e), because both Indiavaí and Nova Guarita
312 poles are still ca. 45° away after rotation from Laurentian and Baltican poles, so the
313 paleomagnetic test of SAMBA also fails in this case too.

314 In the third scenario we tried to minimize the displacement between parts of Amazonia
315 allowing the Colider and Avanavero poles to differ with touching circles of confidence (Fig.
316 5c and f). Even in this case the linearity of the Ventuari-Tapajós province is disrupted, and
317 although Indiavaí and Nova Guarita poles are slightly closer to Laurentian and Baltican poles,
318 there is still a ca. 40° difference.

319 In our opinion, the SAMBA reconstruction is paleomagnetically permissible (but still
320 doubtful) at 1790 Ma, but at 1420 Ma this reconstruction is unlikely. Paleomagnetic
321 reconstructions for 1210–1150 Ma are also inconsistent with the SAMBA hypothesis (Tohver
322 et al., 2002; Elming et al., 2009a).

323 **7. India**

324 The new palaeopole for the 1466 ± 3 Ma Lakhna dykes (Pisarevsky et al., in press; Table
325 1, entry 44) rules out a position of India close to North China (e.g., Zhao et al., 2002, 2004;
326 Zhang et al., 2012). Among other possibilities (which are geologically contradictory, see
327 Pisarevsky et al., in press), this pole, supports the position of India juxtaposed against the
328 southern part of Baltica with the Archean Dharwar and Sarmatia cratons located next to each

329 other, suggesting that they formed part of a single proto-craton (Fig. 6). Sarmatia consists of
330 several Archean terranes which become welded together in the latest Archean – earliest
331 Paleoproterozoic (Bogdanova et al., 1996). The Dharwar Craton has a somewhat similar
332 history with its eastern and western parts welded together at ca 2515 Ma (the age of the
333 ‘stitching’ Closepet Granite, Meert et al., 2010). Late Archean and Paleoproterozoic banded
334 iron formations (BIFs) are widespread both in Sarmatia and Dharwar (Fig. 6; Khan and
335 Naqvi, 1996; Shchipansky and Bogdanova, 1996; Srivastava et al., 2004). Both cratons are
336 bounded by Paleoproterozoic orogenic belts (Fig. 6). The Lipetsk-Losev/East Voronezh Belt
337 probably marks the 2100–2050 Ma accretionary orogen along the eastern margin of Sarmatia,
338 which led to the collision with Volgo-Uralia by 2020 Ma (Schipansky et al., 2007;
339 Bogdanova et al., 2008). Deformation and UHT metamorphism of almost the same age
340 (2040 ± 17 Ma) has been reported from the Satpura Belt, or Central Indian Tectonic Zone
341 (CITZ, Mohanty, 2010). These tectonothermal events reflect some stage of amalgamation of
342 the Dharwar/Bastar/Singhbhum and Bundelkhand/Aravalli cratons. Trends and positions of
343 these two orogens suggest their possible genetic relationship (Fig. 6). Many occurrences of
344 Mesoproterozoic (ca. 1400–1000 Ma) kimberlites and lamproites are reported both from
345 Dharwar and Sarmatia (e.g., Chalapathi Rao et al., 2004; Kumar et al., 2007; Bogatkov et al.,
346 2007). However, many of these bodies are not precisely dated, so no direct correlation is yet
347 possible.

348 An India-Baltica reconstruction (Fig. 6) aligns the eastern margin of India with the
349 southern segment of the west-south western accretionary margin of Baltica. Several
350 discoveries of Palaeo- to Mesoproterozoic ophiolites with ages between 1850 and 1330 Ma in
351 the Eastern Ghats province of India (Fig. 6; Dharma Rao et al., 2011) suggest a long-lived
352 active margin along the eastern Indian margin. This is supported by the development of
353 foreland basins (Biswal et al., 2003; Chakraborty et al., 2010). Geochemical data also suggest

354 subduction-related environments on the eastern Indian margin at 1460 Ma (Pisarevsky et al.,
355 in press).

356 The alignment of Laurentian, Baltican and Indian long-lived Paleo- to Mesoproterozoic
357 accretionary orogens imply a giant, nearly linear, long-lived Paleo- to Mesoproterozoic
358 accretionary orogen comparable in scale to the present eastern Pacific active margin.

359 The timing of India's breakaway from Baltica is not well constrained. Palaeomagnetic data
360 (Table 1, entries 73–75, 93–96) suggest that it occurred between ca. 1120 and 1080 Ma
361 (Pisarevsky et al., in press). There is no evidence of Mesoproterozoic rifting found in the
362 western Dharwar Craton. Such evidence could be concealed in the recently (Cenozoic) rifted
363 away Seychelles Block and/or the Antongil Terrane of Madagascar. However, these blocks
364 were strongly tectonically overprinted in the middle and late Neoproterozoic-Cambrian East
365 African orogen (Tucker et al., 2001; Schofield et al., 2010). Similarly, the south-western
366 margin of Sarmatia is mostly covered and probably strongly overprinted by the Cadomian
367 orogeny. Bogdanova et al. (1996) suggested that the 1300–1100 Ma Volyn-Orsha aulacogen
368 (Fig. 6) could represent the failed arm of a triple junction, which implies that the successful
369 rifting could have occurred along the Teisseyre-Tornquist line, which may also represent
370 rifting between Baltica and India. Poprawa and Paczeńska (2002) suggested that this rifting
371 could have occurred during the Mesoproterozoic. Nikishin et al. (1996), in their 1350–1050
372 Ma paleogeographic reconstruction of Baltica, indicate a continental slope along the
373 Teisseyre-Tornquist line, suggesting the passive continental margin, which could be result of
374 the continental breakup. The 1300–1100 Ma mafic sills in the western part of the Volyn-
375 Orsha aulocogen were mentioned by Bogdanova et al. (2008) with reference to unpublished
376 K-Ar and Rb-Sr dates of Aksenov (1998), which indirectly provide some constraints on the
377 timing of the rifting between Baltica and India.

378 **8. Congo/ São Francisco and Siberia**

379 The Congo/ São Francisco craton is traditionally treated as a single entity, owing to the
380 similarity of Archean and Paleo- to Mesoproterozoic rocks and bounding late Neoproterozoic
381 mobile belts (e.g. Teixeira et al., 2000; Trompette, 1994). Ernst et al. (2013) suggested that
382 the Siberian and Congo/ São Francisco cratons were close to each other between 1500 and
383 1380 Ma. In this case the continuity of general trends of the coeval ca.1500 Ma Kuonamka
384 dyke swarm (Siberia), Curaçá and Chapada Diamantina dyke swarms (São Francisco) and
385 SW Angola sills (Congo) intersect in NE Siberia and provide a possible location for the
386 mantle plume centre (shown in our 1500 Ma reconstruction, Fig.11). There were also coeval
387 1384 ± 2 Ma Siberian Chieress (Ernst et al., 2000) and Congolese Kunene (1385 ± 8 Ma,
388 Drüppel 193 et al., 2000; 1385 ± 25 Ma, Mayer et al., 2004; 1371 ± 3 Ma, McCourt et al.,
389 2004), Kabanga-Musongati-Kapalaglula and Kibaran (1370–1380 Ma, Tack et al., 2000)
390 magmatic events, which support the closeness of these continents for at least 120 m.y. Such a
391 reconstruction is also broadly consistent with two non-key poles – the Siberian 1384 ± 2 Ma
392 Chieress pole (Ernst et al., 2000) and the Angolan 1385–1375 Ma Kunene pole (Piper, 1974,
393 redated by Drüppel et al., 2000; Myer et al., 2004; McCourt et al., 2004; Table 1 entries 62–
394 63). These poles are shown in our 1380 Ma reconstruction (Fig.14). The 1236 ± 24 Ma late
395 Kibaran pole (Meert et al., 1994) also support this reconstruction at later times, as shown in
396 our 1270 Ma reconstruction (Fig.15).

397 **9. Kalahari**

398 Only two poorly dated non-key poorly dated poles are available for Kalahari (Table 1,
399 entries 32 and 37). Pesonen et al. (2003) and Jacobs et al. (2008) showed in their 1770 Ma,
400 1750 Ma and 1200 Ma reconstructions that Kalahari was surrounded by oceans. We follow
401 this suggestion for our 1770–1270 Ma reconstructions where Kalahari is a “lone” continent,
402 the position of which is constrained by the two abovementioned non-key poles.

403 **10. Global paleogeographic reconstructions**

404 Other continents other than those discussed above are paleomagnetically under-
405 represented. For these continents we either used geological constraints to place them in our
406 reconstructions, or in some cases ignored them. All rotation parameters are shown in Table 2.

407 Cratonic cores of most considered continents were formed by the late Paleoproterozoic,
408 but some (Laurentia, Baltica, Amazonia) experienced significant growths during
409 Mesoproterozoic accretionary orogenies. In our reconstructions we schematically showed
410 these growths by increasing the sizes of these continents for successive younger ages (Figs.
411 7–15). Some other continents could also have grown (e.g. Jacobs et al., 2008), but their
412 histories are less certain, so we used the same shape for them during the entire time interval
413 considered.

414 ***10.1. 1770 Ma (Fig. 7)***

415 Several Archean proto-cratons (Superior, Slave, Hearne, Rae, Nain) were interpreted to
416 have collided at ca. 2000–1800 Ma along the Trans-Hudson, Telon-Taltson and Torngat
417 orogens and formed the core of Laurentia (Hoffman, 1989; Karlstrom et al., 2001). Evidence
418 for the 1780–1720 Ma collision between the Wyoming and Hearne cratons, the Big Sky
419 orogeny (Harms et al., 2004), suggests that the Wyoming Craton was approaching Laurentia
420 by 1770 Ma (Fig. 7). The ca. 1800–1700 Ma accretion of juvenile crust along the S-SE
421 Laurentian margin (in present coordinates – hereafter) resulted in the Yavapai orogeny
422 (Karlstrom et al., 2001).

423 The Archean Kola and Karelian cratons collided at the end of the 1940–1860 Ma Lapland-
424 Kola orogeny (Lahtinen et al., 2008) and assembled as the core of Fennoscandia (Bogdanova
425 et al., 2008). At ca. 1920 Ma the accretionary growth of Fennoscandia begun along its SW
426 margin, culminating in the formation of 1810–1770 Ma NW-trending granitoids in southern
427 Sweden, i.e. the older part of the Transscandinavian Igneous Belt (TIB1, Lahtinen et al.,
428 2008).

429 The continuous accretionary orogenic events along the S-SE Laurentian margin and SW
430 Fennoscandian margin suggest an active margin regime along the joint Laurentian-
431 Fennoscandian continent (Pisarevsky and Bylund, 2010). This idea is supported by the ca.
432 1900–1700 Ma Laxfordian orogeny in the northern Scottish blocks of Laurentian affinity
433 (Snyder et al., 1996) and by the active margin conditions in the Makkovik Province of
434 Labrador in the same time interval (Culshaw et al., 2000).

435 The position of the joined Laurentia and Fennoscandia is constrained by paleopoles from
436 both continents (Table 1, entries 1–8; Fig. 7). Sarmatia/India and Volgo-Uralia approached
437 Fennoscandia during that time.

438 Two other building blocks of Baltica – Sarmatia and Volgo-Uralia – have a distinct pre-
439 1800 Ma history and are considered as separate continents up to ca. 2.0 Ga, when they
440 amalgamated (Bogdanova, 1993; Bogdanova et al., 2008). Between 1800 and 1700 Ma
441 Fennoscandia and Volgo-Uralia/Sarmatia approached each other and collided along a suture
442 that was subsequently overprinted by the Volyn-Orsha and Mid-Russian aulacogens
443 (Bogdanova et al., 2008). The 1770–1740 Ma Korosten paleopole from Ukraine (Elming et
444 al., 2001; Elming et al., 2010) suggests that Baltica was not yet assembled at that time. In our
445 reconstruction their position is constrained by the Korosten paleopole and coeval Baltican
446 poles (Table 1, entries 2–6; Fig. 7).

447 Another conglomeration of continents – Australia, Mawson and North China – are loosely
448 constrained by four poles (Table 1, entries 9–12) and geological evidence (see Sections 4 and
449 5).

450 A Siberian connection with Congo/São Francisco is suggested on the basis of previously
451 presented arguments (see Section 8).

452 The position of Amazonia/West Africa is constrained by two poles (Table 1, entries 13
453 and 15). However, the Colider pole (Table 1, entry 14) is not supportive of this position (see

454 discussion in Section 6). Accretion continued along the SW margin of Amazonia, expressed
455 by the 1780–1550 Ma Rio Negro – Juruena province.

456 There are indicators of subduction under the western margin of Kalahari and of a passive
457 regime on its eastern margin (Jacobs et al., 2008), which suggest that this continent was
458 surrounded by oceans.

459 ***10.2. 1720 Ma (Fig. 8)***

460 Laurentia’s SE margin grew during the Yavapai accretionary orogeny, and accretion
461 continued during the Mazatzal-Labrador orogeny. The Wyoming Craton collided with the
462 Hearne Craton (the Big Sky orogeny), and Sarmatia-India and Volgo-Uralia moved closer to
463 Fennoscandia. The position of Laurentia-Fennoscandia is constrained by the Cleaver Dykes
464 pole (Irving et al., 2004; Table 1, entry 20), whereas there is no coeval pole for Fennoscandia.

465 An equatorial position of Siberia is supported by recently published poles from the Aldan
466 block (Didenko et al., 2013; Table 1, entries 24–25) and three non-key VGPs (Table 1,
467 entries 21–23).

468 The position and orientation of Australia is well constrained paleomagnetically (Table 1,
469 entries 16–19). Accretionary processes continued along the southern margin of the NAC
470 (1740–1715 Ma Strangways orogeny; Betts and Giles, 2006).

471 The location and orientation of Amazonia/West Africa is uncertain. In this and several
472 further reconstructions we place them into positions interpolated from paleomagnetically
473 constrained 1770 Ma and 1420 Ma reconstructions.

474 ***10.3. 1650 Ma (Fig. 9)***

475 The position of the Laurentia-Baltica is constrained by two Baltican poles (Table 1, entries
476 26–27). Accretion along SE Laurentia (the Mazatzal orogeny), W Baltica (the Gothian
477 orogeny) and India continued.

478 Australia/Mawson approached western Laurentia at this time (the first phase of the
479 Racklan orogeny). Accretion along the southern margin of the NAC continued (the Liebig
480 Event; Betts and Giles, 2006).

481 Siberia was moving closer to its paleomagnetically constrained 1470 Ma position, and the
482 position of Kalahari is loosely constrained by two non-key poles (Table 1, entries 32 and 37).

483 ***10.4. 1580 Ma (Fig. 10)***

484 The position of the Laurentia-Baltica is constrained by two Baltican poles (Table 1, entries
485 33–34). The accretion along the SW Laurentian margin temporarily stopped (Karlstrom et al.,
486 2001). However, accretion continued along the western Baltican (the Gothian orogeny) and
487 possibly the SE Indian margins.

488 At ca. 1600 Ma a collision between the NAC and Laurentia occurred, and their relative
489 positions are also paleomagnetically constrained (Table 1, entries 35–36). Betts et al. (2007)
490 reported a 1600–1500 Ma hot spot track from SAC to NAC. The position of the suggested
491 mantle plume head is shown in this and the next reconstructions.

492 We speculate that ca. 1600–1580 Ma was the time of the complete assembly of Nuna
493 when two continental assemblies – Laurentia-Baltica-India (West Nuna) and Australia-
494 Mawson-North China (East Nuna) – amalgamated. It is not clear whether Siberia-Congo/São
495 Francisco also joined Nuna at the same time, or if this occurred later, at ca. 1500–1470 Ma
496 (see Section 3).

497 The position of Kalahari, which we suggest was a “lone”, continent is loosely constrained
498 by a non-key pole (Table 1, entry 37).

499 ***10.5. 1500 Ma (Fig. 11)***

500 The position of Laurentia-Baltica is constrained by two Baltican poles (Table 1, entries
501 38–39). Tectonic activity (Pinwarian orogeny) was renewed along the NE Laurentian margin
502 involving subduction beneath Laurentia (Karlstrom et al., 2001 and references therein; Gower

503 and Krogh, 2002). The 1520–1480 Ma Telemarkian accretion continued along the western
504 margin of Baltica (Bingen et al., 2008).

505 Nuna moved northward and the NAC moved across the mantle plume (Betts et al., 2007).
506 Another mantle plume possibly reached the surface in NE Siberia, causing the Kuonamka-
507 Curaçá-Chapada Diamantina radial dyke swarm (see Section 8).

508 ***10.6. 1470–1450 Ma (Fig. 12 and 13)***

509 During this time interval the position of the Laurentia-Baltica continent is well constrained
510 by paleomagnetic data (Table 1, entries 45–52).

511 The tectonic regime along the SE margin of Laurentia is generally regarded as
512 ‘anorogenic’ (e.g., Davidson, 2008 and references therein), but there is some evidence for
513 continental arc magmatism and collision of ca. 1500–1400 Ma juvenile crustal blocks
514 (Karlstrom et al., 2001 and references therein). Gower and Krogh (2002) explained the 1460–
515 1230 Ma Elsonian magmatism in the Genville Province by a low angle subduction, possibly
516 associated with an overridden spreading centre. Accretion also continued along the western
517 margin of Baltica (the 1470–1420 Ma Hallandian-Danopolonian orogeny; Bingen et al.,
518 2008).

519 The westerly source region for of Paleoproterozoic detritus in the Belt-Purcell
520 sedimentary basin near the western margin of Laurentia (Fig. 13) is distinct from known
521 Laurentian crust (e.g. Davidson, 2008 and references therein). The tectonic setting of this
522 basin has been debated (e.g. Hoffman, 1989; Winston and Link, 1993 and references therein),
523 however, most workers argued in favour of an intracontinental origin (e.g. Davidson, 2008).
524 We suggest that the Belt-Purcell basin developed on the failed arm of a rifting system (Fig.
525 13). Rifting was probably related to the 1469–1457 Ma Moyie sills found in the lower part of
526 the Belt Supergroup (Elston et al., 2002). Traces of ca. 1450–1430 Ma magmatism are also
527 found in Hainan Island (Cathasia), which could have been a part of Laurentia during the late

528 Paleo- to Mesoproterozoic (Li et al., 2008a,b). In our model two successive rifting arms
529 caused a separation of the Mawson/Gawler part of East Nuna from Laurentia (Fig. 13).

530 *10.7. 1380 Ma (Fig. 14)*

531 The rifting between western Laurentia and Mawson/SAC propagated northward (present
532 coordinates) and eventually caused the breakup between the NAC and Laurentia at ca. 1380
533 Ma (the age of the Hart River magmatism).

534 This propagating rifting caused internal movements within East Nuna, in particular the
535 anticlockwise rotation of the SAC with respect to the NAC (Figure 18a of Betts and Giles,
536 2006) caused the separation of the Mount Isa Inlier (NAC) from the Broken Hill area (SAC)
537 and closure of the gap between SAC and WAC marking the initial stage of the Albany-Fraser
538 orogeny.

539 On the basis of a new ca. 1350 Ma pole from North China, breakup and rotation of this
540 continent from East Nuna after ca. 1400 Ma is suggested (Table 1, entry 61).

541 The position of Laurentia-Baltica is supported paleomagnetically (Table 1, entries 56–60).
542 The SE margin of Laurentia was probably still subduction-related (e.g., Rivers, 1997 and
543 references therein; Karlstrom et al., 2001 and references therein; Gower and Krogh, 2002),
544 whereas it is less certain along the western margin of Baltica. Bingen et al. (2008) described
545 the 1340–1140 Ma Pre-Sveconorwegian interval for western Baltica as “an extensional or
546 transtensional regime located in a continental arc, continental back-arc or Basin and Range
547 environment”. The eastern Indian margin was probably also active as Dharma Rao et al.
548 (2001) reported a ca. 1330 Ma Kanigiri ophiolitic mélange in that area.

549 The fixed distal position of Siberia with respect to Laurentia (see Section 3) is also
550 supported by a match between the non-key 1384 ± 2 Ma Chieress VGP and coeval
551 Laurentian poles (Table 1, entries 56–60 and 62).

552 The Siberian connection with Congo/São Francisco (see Section 8) is supported by the
553 mentioned Chieress pole and the non-key 1385–1375 Ma Kunene pole (Table 1, entry 63).

554 **10.8. 1270 Ma (Fig. 15)**

555 The paleoposition of Laurentia is paleomagnetically well constrained (Table 1, entries 65–
556 71), and the Baltican pole from post-Jotnian Intrusions suggest that Baltica and Laurentia still
557 were still connected (Table 1, entry 64). The Elzevirian orogeny continued along the NE
558 margin of Laurentia (e.g. Davidson, 2008 and references therein).

559 Although there are no Australian paleomagnetic data for this time, we suggest that
560 Australia was widely separated from Laurentia, as indicated by younger paleopoles from both
561 continents (Table 1, entries.67, 76 and 90).

562 The slightly younger, 1260–1212 Ma, late Kibaran pole from Congo (Table 1, entry 72)
563 suggests that the Siberian connection with Congo/São Francisco still persisted.

564 **11. Final remarks**

565 After the ca. 2.0–1.8 Ga assemblies of most proto-continent – Laurentia, Fennoscandia,
566 Sarmatia/Volgo-Uralia, Siberia, NAC, WAC, SAC/Mawson, North China, Congo/São
567 Francisco, Amazonia/West Africa, India and Kalahari – some of these collided to form two or
568 three stable continental masses by ca. 1700 Ma. The first landmass, that we preliminary call
569 West Nuna, consisted of Laurentia, Baltica (Fennoscandia/Sarmatia/Volgo-Uralia) and
570 probably India. The second landmass (East Nuna) included North, West and South Australia,
571 the Mawson craton of Antarctica and North China. Although these two land masses may have
572 joined as a single supercontinent by ca. 1.75 Ga as suggested by numerous previous studies
573 (e.g., Zhao et al., 2004, 2004; Evans and Mitchell, 2011; Zhang et al., 2012), such a
574 connection may not have been stable and some minor relative movements might have
575 occurred between them after this time but prior to ca. 1600. We suggest that East and West
576 Nunas likely collided between 1650 and 1580 Ma to form a more coherent Nuna

577 supercontinent. Siberia and possibly Congo/São Francisco joined Nuna at ca. 1500 Ma, if not
578 earlier. The breakup of Nuna occurred between ca. 1450 and 1380 Ma. The first stage of this
579 separation caused internal displacements within East Nuna – rotation of SAC/Mawson with
580 respect to NAC and WAC. North China also broke away from East Nuna. By 1270 Ma a
581 wide ocean had developed between West and East Nunas. West Nuna, Siberia (connected
582 with northern Laurentia by as yet unknown continental blocks) and maybe Congo/São
583 Francisco remained a single continent until ca. 1270 Ma. It is yet unclear whether
584 Amazonia/West Africa and Kalahari were ever parts of Nuna.

585 **Acknowledgments**

586 This work was initiated at the Nordic Palaeomagnetic Workshop held in Luleå in 2009. The
587 authors thank the participants in the workshop for their contributions to the discussions on a
588 global palaeomagnetic database commonly accepted reliable to be used for tectonic
589 reconstructions. We thank two anonymous reviewers for their suggestions and corrections
590 which improved the manuscript. The paleogeographic reconstructions are made with free
591 GPLATES software (<http://www.gplates.org/>). This is contribution 309 from the ARC Centre
592 of Excellence for Core to Crust Fluid Systems (<http://www.ccfs.mq.edu.au>) and TIGeR
593 publication #465. SAE thanks the Swedish Research Council for their financial support.

594 **Appendix**

595 An animated history, 1770–1270 Ma – PowerPoint animation available at (link to the
596 PowerPoint file at the Elsevier online version).

597

598 **References**

599 Abrahamsen, N., Van der Voo, R., 1987. Palaeomagnetism of middle Proterozoic (c.1.25
600 Ga) dykes from central North Greenland. *Geophysical Journal of the Royal Astronomic*
601 *Society* 91, 597-611.

602 Aksenov, E.M., 1998. The Geological Evolution of the East European Craton in the Late
603 Proterozoic. Institute of Precambrian Geology and Geochronology, St. Petersburg, Russia,
604 Summary of Doctor Sciences' thesis, 106 pp. (in Russian).

605 Åhäll, K-I., Connelly, J.N., 2008. Long-term convergence along SW Fennoscandia: 330
606 m.y. of Proterozoic crustal growth. *Precambrian Res.* 163, 402-421.

607 Baker, M.J., Crawford, A.J., Withnall, I.W., 2010. Geochemical, Sm-Nd isotopic
608 characteristics and petrogenesis of Paleoproterozoic mafic rocks from the Georgetown
609 Inlier, north Queensland: implications for relationship with the Broken Hill and Mount Isa
610 Eastern Succession. *Precambrian Research* 177, 39-54.

611 Betts, P.G., Giles, D., 2006. The 1800-1100 Ma tectonic evolution of Australia.
612 *Precambrian Research* 144, 92-125.

613 Betts, P. G., Giles, D., Schaefer, B. F., Mark, G., 2007. 1600–1500 Ma hotspot track in
614 eastern Australia: implications for Mesoproterozoic continental reconstructions. *Terra Nova*
615 19, 496-501.

616 Betts, P. G., Giles, D., Schaefer, B. F., 2008. Comparing 1800 – 1600 Ma accretionary and
617 basin processes in Australia and Laurentia: Possible geographic connections in Columbia,
618 *Precambrian Research* 166, 81 – 92

619 Betts, P. G., Giles, D., Foden, J., Schaefer, B. F., Mark, G., Pankhurst, M.J., Forbes, C.J.,
620 Williams, H.A., Chalmers, N.C., Hills, Q., 2009. Mesoproterozoic plume-modified
621 orogenesis in eastern Precambrian Australia. *Tectonics* 28, TC3006,
622 doi:10.1029/2008TC002325.

623 Bingen, B., Andersson, J., Söderlund, U., Möller, C., 2008. The Mesoproterozoic in the
624 Nordic countries. *Episodes* 31(1), 29-34.

625 Bispo-Santos, F., D'Agrella-Filho, M.S., Pacca, I.I.G., Janikian, L., Trindade, R.I.F.,
626 Elming, S.-Å., Silva, J.A., Barros, M.A.S., Pinho, F.E.C., 2008. Columbia revisited:

627 paleomagnetic results from the 1790 Ma Colíder volcanic (SW Amazonian Craton, Brazil).
628 *Precambrian Res.* 164, 40–49.

629 Bispo-Santos, F., D'Agrella-Filho, M.S., Trindade, R.I.F., M.S., Elming, S.-Å., Janikian,
630 L., Vaconcelos, P.M., Perillo, B.M., Pacca, I.I.G., da Silva, J.A., Barros, M.A.S., 2012.
631 Tectonic implications of the 1419 Ma Nova Guarita mafic intrusives paleomagnetic pole
632 (Amazonian Craton) on the longevity of Nuna. *Precambrian Research* 196-197, 1-22.

633 Biswal, T.K., Sinha, S., Mandal, A., Ahuja, H., Das, M.K., 2003. Deformation pattern of
634 Bastar craton adjoining Eastern Ghat mobile belt, NW Orissa. *Gondwana Geological*
635 *Magazine, Special Publication* 7, 101–108.

636 Bogatikov, O.A., Kononova, V.A., Nosova, A.A., Kondrashov, I.A., 2007. Kimberlites
637 and lamproites of the east European Platform: petrology and geochemistry. *Petrology* 15(4),
638 315-334.

639 Bogdanova, S.V., 1993. Segments of the East European Craton. In: Gee, D.G.,
640 Beckholmen, M. (Eds.), *EUROPROBE in Jablonna 1991*. European Science Foundation,
641 Polish Academy of Sciences, pp. 33–38.

642 Bogdanova, S.V., Pashkevich, I.K., Gorbatshev, R., Orlyuk, M., 1996. Riphean rifting
643 and major Paleoproterozoic boundaries in the East European Craton: geology and geophysics.
644 *Tectonophysics* 268, 1–22.

645 Bogdanova, S. V., Page, L. M., Skridlaite, G., Taran, L. N., 2001. Proterozoic
646 tectonothermal history in the western part of the East European Craton: $^{40}\text{Ar}/^{39}\text{Ar}$
647 geochronological constraints: *Tectonophysics* 339, 39–66.

648 Bogdanova, S. V., Bingen, B., Gorbatshev, R., Kheraskova, T. N., Kozlov, V. I.,
649 Puchkov, V. N., Volozh, Yu. A., 2008. The East European Craton (Baltica) before and during
650 the assembly of Rodinia. *Precambrian Research* 160, 23–45.

651 Boger, S.D., 2011. Antarctica – before and after Gondwana. *Gondwana research* 19, 335-
652 371.

653 Brookfield, M.E., 1993. Neoproterozoic Laurentia-Australia fit. *Geology* 21, 683-686.

654 Buchan, K. L., Halls, H. C., 1990. Paleomagnetism of Proterozoic mafic dyke swarms of
655 the Canadian Shield. In: Parker, A. J., Rickwood, P. C., Tucker, D. H. (eds), *Mafic Dykes
656 and Emplacement Mechanism: Rotterdam, A. A. Balkema*, pp. 209–230.

657 Burrett, C., Berry, R., 2000. Proterozoic Australia-Western United States (AUSWUS) fit
658 between Laurentia and Australia. *Geology* 28, 103-106.

659 Bylund, G., 1985. Palaeomagnetism of middle Proterozoic basic intrusives in central
660 Sweden and the Fennoscandian apparent polar wander path. *Precambrian Research* 28,
661 283-310.

662 Cawood, P.A., Korsch, R.J., 2008. Assembling Australia: Proterozoic building of a
663 continent. *Precambrian Research* 166, 1–38

664 Chakraborty, P.P., Dey, S., Mohanty, S.P., 2010. Proterozoic platform sequences in
665 Peninsular India: Implications towards basin evolution and supercontinent assembly. *J. Asian
666 earth Sci.* 39, 589-607.

667 Chalapathi Rao, N.V., Gibson, S.A., Pyle, D.M., Dickin, A.P., 2004. Petrogenesis of
668 Proterozoic Lamproites and Kimberlites from the Cuddapah Basin and Dharwar Craton,
669 Southern India. *J. Petrology* 54, 907-948.

670 Chen, L., Huang, B., Yi, Z., Zhao, J., Yan, Y., 2013. Paleomagnetism of ca. 1.35 Ga sills
671 in northern North China Craton and implications for paleogeographic reconstruction of the
672 Mesoproterozoic supercontinent. *Precambrian Research* 228, 36-47.

673 Cook, F.A., Erdmer, P., 2005. An 1800 km cross section of the lithosphere through the
674 northwestern North American plate: lessons from 4.0 billion years of Earth's history. *Can. J.
675 Earth Sci.* 42, 1295-1311.

676 Cook, F.A., Clowes, R.M., Snyder, D.B., van der Velden, A.J., Hall, K.W., Erdmer, P.,
677 Evenchick, C.A., 2004. Precambrian crust beneath the Mesozoic northern Canadian Cordillera
678 discovered by Lithoprobe seismic reflection profiling. *Tectonics* 23, TC2010.

679 Culshaw, N., Ketchum, J., Barr, S., 2000. Structural evolution of the Makkovik Province,
680 Labrador, Canada: Tectonic processes during 200 Myr at a Paleoproterozoic active margin.
681 *Tectonics* 19, 961-977.

682 D'Agrella-Filho, M.S., Trindade, R.I.F., Elming, S-Å., Teixeira, W., Yokoyama, E.,
683 Tohver, E., Geraldes, M.C., Pacca, I.I.G., Barros, M.A.S., Ruis, A.S., 2012. The 1420 Ma
684 Indiavaí Mafic Intrusion (SW Amazonian Craton): Paleomagnetic results and implications for
685 the Columbia supercontinent. *Gondwana Research* 22, 956-973.

686 Dalziel, I.W.D., 1991. Pacific margins of Laurentia and East Antarctica–Australia as a
687 conjugate rift pair: evidence and implications for an Eocambrian supercontinent. *Geology* 19,
688 598–601.

689 Davidson, A., 2008. Late Paleoproterozoic to mid-Neoproterozoic history of northern
690 Laurentia: an overview of central Rodinia. *Precambrian Research* 160, 5-22.

691 Davis, D.W., Paces, J.B., 1990. Time resolution of geologic events on the Keweenaw
692 Peninsula and applications for development of the Midcontinent Rift system. *Earth and*
693 *Planetary Science Letters*, 97 54-64.

694 Dharma Rao, C.V., Santosh, M., Wu, Y-B., 2011. Mesoproterozoic ophiolitic mélange
695 from the SE periphery of the Indian plate: U-Pb zircon ages and tectonic implications.
696 *Gondwana Research* 19, 384-401.

697 Didenko, A.N., Kozakov, I.K., Dvorova, A.V., 2009. Paleomagnetism of granites from the
698 Angara-Kan basement inlier, Siberian craton. *Russian Geology and Geophysics* 50, 57–62.

699 Didenko, A.N., Peskov, A.Yu., Guryanov, V.A., Perestoronin, A.N., Kosynkin, A.V.,
700 2013. Paleomagnetism of the Ulkan trough (SE of Siberian craton). *Tikhookeanskaia*
701 *Geologia* 32(1), 32–55 (in Russian).

702 Diehl, J.F., Haig, T.D., 1994. A paleomagnetic study of the lava flows within the Copper
703 Harbour Conglomerate, Michigan: new results and implications. *Canadian Journal of Earth*
704 *Sciences* 31, 369-380.

705 Drüppel, K., Littmann, S., Okrusch, M., 2000. Geo und intrusi- chemische Unter-
706 suchungen Anorthosite des Kunene-Intrusiv-Komplex (KIC) in NW-Namibia. *European*
707 *Journal Mineralogy* 12, 37.

708 Elming, S.-Å., Mattsson, H., 2001. Post Jotnian basic Intrusions in the Fennoscandian
709 Shield, and the break up of Baltica from Laurentia: a palaeomagnetic and AMS study.
710 *Precambrian Research* 108, 215-236.

711 Elming, S.-Å., Pesonen, L.J., 2010. Recent Developments in Paleomagnetism and
712 Geomagnetism. Sixth Nordic Paleomagnetic Workshop, Luleå (Sweden), 15-22 September
713 2009. *EOS*, 90 (51) 502.

714 Elming, S.-Å., Shumlyanskyy, L., Kravchenko, S., Layer, P., Söderlund, U., 2010.
715 Proterozoic basic dykes in the Ukrainian Shield: A palaeomagnetic, geochronologic and
716 geochemical study – The accretion of the Ukrainian Shield to Fennoscandia. *Precambrian*
717 *Research* 178, 119 – 135.

718 Elming, S.-Å., D’Agrella-Filho, M.S., Page, L.M., Tohver, E., Trindade, R.I.F., Pacca,
719 I.I.G., Geraldes, M.C., Teixeira, W., 2009a. A palaeomagnetic and $^{40}\text{Ar}/^{39}\text{Ar}$ study of late
720 Precambrian sills in the SW part of the Amazonian craton: Amazonia in the Rodinia.
721 *Geophysical Journal International* 178, 106-122.

722 Elming, S.-Å., Moakhar, M.O., Layer, P., Donadini, F., 2009b. Uplift deduced from
723 remanent magnetization of a proterozoic basic dyke and the baked country rock in the Hoting

724 area, Central Sweden: a palaeomagnetic and $^{40}\text{Ar}/^{39}\text{Ar}$ study. *Geophysical Journal*
725 *International* 179, 59-78.

726 Elming, S.-Å., Mikhailova, N. P., Kravchenko, S., 2001, Palaeomagnetism of Proterozoic
727 rocks from the Ukrainian Shield: new tectonic reconstructions of the Ukrainian and
728 Fennoscandian shields: *Tectonophysics* 339, 19–38.

729 Elston, D.P., Enkin, R.J., Baker, J., Kisilevsky, D.K., 2002. Tightening the Belt:
730 Paleomagnetic-stratigraphic constraints on deposition, correlation, and deformation of the
731 Middle Proterozoic (ca. 1.4 Ga) Belt-Purcell Supergroup, United States and Canada. *GSA*
732 *Bulletin* 114, 619-638.

733 Emslie, R.F., Irving, E., Park, J.K., 1976. Further paleomagnetic results from the
734 Michikamau Intrusion, Labrador. *Canad. J. Earth Sci.* 13, 1052-1057.

735 Ernst, R.E., Buchan, K.L., 1993. Paleomagnetism of the Abitibi dyke swarm, southern
736 Superior Province, and implications for the Logan Loop. *Canad. J. Earth Sci.* 30, 1886-1897.

737 Ernst, R.E., Buchan, K.L., Hamilton, M.A., Okrugin, A.V., Tomshin, M.D., 2000.
738 Integrated paleomagnetism and U–Pb geochronology of mafic dikes of the Eastern Anabar
739 shield region, Siberia: implications for Mesoproterozoic paleolatitude of Siberia and
740 comparison with Laurentia. *Journal of Geology* 108, 381–401.

741 Ernst, R.E., Pereira, E., Hamilton, M.A., Pisarevsky, S.A., Rodrigues, J., Tassinari,
742 C.C.G., Teixeira, W., Van-Dunem, V., 2013. Mesoproterozoic intraplate magmatic ‘barcode’
743 record of the Angola portion of the Congo Craton: Newly dated magmatic events at 1500 and
744 1110 Ma and implications for Nuna (Columbia) supercontinent reconstructions. *Precambrian*
745 *Research* 230, 103-118.

746 Evans, D.A.D., Pisarevsky, S.A., 2008. Plate tectonics on the early Earth?-weighing the
747 paleomagnetic evidence. In: Condie, K. & Pease, V. (eds). *When Did Plate Tectonics Begin?*
748 *Geological Society of America Special Paper* 440, 249-263.

749 Evans, D.A.D., Mitchell, R.N., 2011. Assembly and breakup of the core of
750 Paleoproterozoic–Mesoproterozoic supercontinent Nuna. *Geology* 39, 443-446.

751 Fahrig, W.F., Jones, D.L., 1976. The paleomagnetism of the Helikian Mistatin pluton,
752 Labrador, Canada. *Canad. J. Earth Sci.* 13, 832-837.

753 Fanning, C.M., Dally, S.J., Bennett, V.C., Ménot, R.P., Peucat, J.J., Oliver, G.J.H.,
754 Monnier, O., 1995. The “Mawson Block”: once contiguous Archaean to Proterozoic crust in
755 the East Antarctic Shield and the Gawler Craton. In: Ricci, C.A. (Ed.), *Abstracts*, 7th
756 International Symposium on Antarctic Earth Sciences, Sienna.

757 Fedotova, M. A., Khramov, A. N., Pisakin, B. N., Priyatkin, A. A., 1999. Early
758 Proterozoic palaeomagnetism: new results from the intrusive and related rocks of the
759 Karelian, Belomorian and Kola provinces, eastern Fennoscandian Shield. *Geophysical*
760 *Journal International* 137, 691–712

761 Fitzsimons, I.C.W. 2003. Proterozoic basement provinces of southern and southwestern
762 Australia, and their correlation with Antarctica. In: Yoshida, M., Windley, B., Dasgupta, S.
763 (eds). *Proterozoic East Gondwana: supercontinent assembly and breakup*. Geological Society
764 of London Special Publication No 206, 93-130.

765 Fraser, G.L., Huston, D.L., Gibson, G.M., Neumann, N.L., Maidment, D., Kositcin, N.,
766 Skirrow, R.G., Jaireth, S., Lyons, P., Carson, C., Cutten, H., Lambeck, A., 2007. Geodynamic
767 and metallogenic evolution of Proterozoic Australia from 1870 – 1550 Ma: a discussion.
768 *Geoscience Australia Record* 2007/16.

769 Fuck, R.A., Brito Neves, B.B., Schobbenhaus, C., 2008. Rodinia descendants in South
770 America. *Precambrian Research* 160, 108-126.

771 Furlanetto, F., Thorkelson, D.J., Gibson, H.D., Marshall, D.D., Rainbird, R.H., Davis,
772 W.J., Crowley, J.L., Vervoort, J.D., 2013. Late Paleoproterozoic terrane accretion in

773 northwestern Canada and the case for circum-Columbian orogenesis. *Precambrian Research*
774 224, 512-528.

775 Gala, M.G., Symons, D.T.A., Palmer, H.C., 1995. Paleomagnetism of the Jan Lake
776 Granite, Trans-Hudson Lake Orogen. *Saskatchewan Geol. Surv. Misc. Rpt.*, 95-4.

777 Gallet, Y., Pavlov, V.E., Semikhatov, M.A., Petrov, P.Yu., 2000. Late Mesoproterozoic
778 magnetostratigraphic results from Siberia: paleogeographic implications and magnetic field
779 behaviour. *Journal of Geophysical Research* 105, 16481-16499.

780 Gibson, G.M., Rubenach, M.J., Neumann, N.L., Southgate, P.N., Hutton, L.J., 2008. Syn-
781 and post-extensional tectonic activity in the Palaeoproterozoic sequences of Broken Hill and
782 Mount Isa and its bearing on reconstructions of Rodinia. *Precambrian Research*

783 Giles, D., Betts, P., Lister, G., 2002. Far-field continental backarc setting for the 1.80-1.67
784 Ga basins of northeastern Australia. *Geology* 30, 823-826.

785 Gladkochub, D.P., Wingate, M.T.D., Pisarevsky, S.A., Donskaya, T.V., Mazukabzov,
786 A.M., Ponomarchuk, V.A., Stanevich, A.M., 2006. Mafic intrusions in southwestern Siberia
787 and implications for a Neoproterozoic connection with Laurentia. *Precambrian Research* 147,
788 260-278.

789 Gladkochub, D.P., Pisarevsky, S.A., Donskaya, T.V., Ernst, R.E., Wingate, M.T.D.,
790 Söderlund, U., Mazukabzov, A.M., Sklyarov, E.V., Hamilton, M.A., Hanes, J.A., 2010.
791 Proterozoic mafic magmatism in Siberian craton: an overview and implications for
792 paleocontinental reconstruction. *Precambrian Research* 183, 660-668,

793 Goodge, J.W., Vervoort, J.D., Fanning, C.M., Brecke, D.M., Farmer, G.L., Williams, I.S.,
794 Myrow, P.M., DePaolo, D.J., 2008. A positive test of East Antarctica – Laurentia
795 juxtaposition within the Rodinia supercontinent. *Science* 321, 235-240.

796 Gorbatshev, R., Bogdanova, S., 1993. *Frontiers in the Baltic Shield*. *Precambrian Res.* 64,
797 3–21.

798 Gower, C.F., Krogh, T.E., 2002. A U–Pb geochronological review of the Proterozoic
799 history of the eastern Grenville Province. *Can. J. Earth Sci.* 39, 795–829.

800 Gower, C. F., Ryan, A. B., Rivers, T., 1990. Mid-Proterozoic Laurentia-Baltica: an
801 overview of its geological evolution and a summary of the contributions made by this
802 volume. In Gower, C. F., Rivers, T., Ryan, B. (eds), *Mid-Proterozoic Laurentia-Baltica:*
803 *Geological Association of Canada, Special Paper 38*, 1–20.

804 Gregory, L.C., Meert, J.G., Pradhan, V., Pandit, M.K., Tamrat, E., Malone, S.J., 2006. A
805 paleomagnetic and geochronological study of the Majhgawan Kimberlite, India: implications
806 for the age of the Vindhyan SuperGroup. *Precambrian Research* 149, 65–75.

807 Gurevich, E.L., 1984. Paleomagnetism of the Ordovician deposits of the Moyero river
808 sequence. *Paleomagnetic methods in stratigraphy*. VNIGRI, St. Petersburg, pp. 35–41 (in
809 Russian).

810 Halls, H.C., Li, J., Davis, D., Hou, G., Zhang, B., Qian, X., 2000. A precisely dated
811 Proterozoic palaeomagnetic pole for the North China craton, and its relevance to
812 palaeocontinental reconstruction. *Geophys. J. Int.* 143, 185-203.

813 Hamilton, M.A., Buchan, K.L., 2010. U–Pb geochronology of the Western Channel
814 Diabase, northwestern Laurentia: Implications for a large 1.59 Ga magmatic province,
815 Laurentia’s APWP and paleocontinental reconstructions of Laurentia, Baltica and Gawler
816 craton of southern Australia. *Precambrian Research* 183, 463-473.

817 Hargraves, R.B., 1989. Paleomagnetism of Mesozoic kimberlites in Southern Africa and
818 the Cretaceous apparent polar wander curve for Africa. *J. Geophys. Res.* 94, 1851–1866.

819 Harlan, S.S., Geissman, J.W., Snee, L.W., 2008. Paleomagnetism of Proterozoic mafic
820 dikes from the Tobacco Root Mountains, southwest Montana. *Precambrian Research* 163,
821 239-264.

822 Harms, T.A., Brady, J.B., Burger, H.R., Cheney, J.T., 2004. Advances in the geology of
823 the Tobacco Root Mountains, Montana, and their implications for the history of the northern
824 Wyoming province. In: Brady, J.B., Burger, H.P., Cheney, J.T., Harms, T.A. (eds),
825 Precambrian geology of the Tobacco Root Mountains, Montana. Boulder, Colorado,
826 Geological Society of America Special Paper 377, 227-243.

827 He, Y.H., Zhao, G.C., Sun, M., 2010. Geochemical and isotopic study of the Xiong'er
828 volcanic rocks at the southern margin of the North China Craton: Petrogenesis and tectonic
829 implications. *Journal of Geology* 118, 417–433.

830 Henry, S.G., Mauk, F.J., Van der Voo, R., 1977. Paleomagnetism of the upper
831 Keweenawan sediments: the Nonesuch Shale and Freda Sandstone. *Canadian Journal of*
832 *Earth Sciences* 14, 1128-1138.

833 Hildebrand, R.S., Hoffman, P.F., Bowring, S.A., 2010. The Calderian orogeny in Wopmay
834 orogen (1.9 Ga), northwestern Canadian Shield. *GSA Bulletin* 122, 794-814.

835 Hoffman, P. F., 1997. Tectonic genealogy of North America. In Van der Pluijm, B. A.
836 And Marshak, S. (Eds), *Earth Structure, an Introduction to Structural Geology and Tectonics:*
837 *New York, McGraw Hill, p. 459–464.*

838 Hoffman, P.F., 1989. Precambrian geology and tectonic history of North America. In:
839 Bally, A.W., Palmer, A.R. (eds), *The Geology of North America – an overview.* Boulder,
840 Colorado, Geological Society of America, *The Geology of North America A*, pp. 447-512.

841 Idnurm, M., 2000. Towards a high resolution Late Palaeoproterozoic – earliest
842 Mesoproterozoic apparent polar wander path for northern Australia. *Aust. J. Earth Sci.* 47,
843 405-429.

844 Idnurm, M., Giddings, J.W., Plumb, K.A., 1995. Apparent polar wander and reversal
845 stratigraphy of the Palaeo-Mesoproterozoic southeastern McArthur Basin, Australia.
846 *Precambrian Research* 72, 1-41.

847 Irving, E., Donaldson, J.A., Park, J.K., 1972. Paleomagnetism of the Western Channel
848 Diabase and associated rocks, Northwest Territories. *Canad. J. Earth Sci.* 9, 960-971.

849 Irving, E., Baker, J., M. Hamilton, M., Wynne, P.J., 2004. Early Proterozoic geomagnetic
850 field in western Laurentia: implications for paleolatitudes, local rotations and stratigraphy.
851 *Precambrian Research* 129, 251-270.

852 Jacobs, J., Pisarevsky, S.A., Thomas, R.J., Becker T., 2008. The Kalahari Craton during
853 the assembly and dispersal of Rodinia. *Precambrian Research* 160, 142-158.

854 Johansson, Å., 2009. Baltica, Amazonia and the SAMBA connection -1000 million years
855 of neighbourhood during the Proterozoic? *Precambrian Res.* 175, 221–234.

856 Jones, D.L., McElhinny, M.W., 1966. Paleomagnetic correlations of basic intrusions in the
857 Precambrian of southern Africa. *J. Geophys. Res.* 71, 543–552.

858 Karlstrom, K.E., Harlan, S.S., Åhäll, K.I., Williams, M.L., McLelland, J., Geissman, J.W.,
859 2001. Long-lived (1.8–1.0 Ga) convergent orogen in southern Laurentia, its extensions to
860 Australia and Baltica, and implications for refining Rodinia. *Precambrian Res.* 111, 5–30.

861 Khan, R.M.K., Naqvi, S.M., 1996. Geology, geochemistry and genesis of BIF of Kushtagi
862 schist belt, Archaean Dharwar Craton, India. *Mineral. Deposita* 31, 123-133.

863 Kumar, A., Heaman, L.M., Manikyamba, C., 2007. Mesoproterozoic kimberlites in south
864 India: a possible link to ~1.1 Ga global magmatism. *Precambrian Res.* 154, 192-204.

865 Lahtinen, R., Garde, A.A., Melezhik, V.A., 2008. Paleoproterozoic evolution of
866 Fennoscandia and Greenland. *Episodes* 31(1), 20-28.

867 LeCheminant, A. N., Heaman, L. M., 1989. MacKenzie igneous events, Canada: Middle
868 Proterozoic hotspot magmatism associated with ocean opening. *Earth and Planetary Science*
869 *Letters* 96, 38–48.

870 Li, Z.X., Evans, D.A.D., 2011. Late Neoproterozoic 40° intraplate rotation within
871 Australia allows for a tighter-fitting and longer-lasting Rodinia. *Geology* 39, 39-42.

872 Li, Z.X., Zhang, L., Powell, C.M., 1995. South China in Rodinia: part of the missing link
873 between Australia–East Antarctica and Laurentia? *Geology* 23, 407–410.

874 Li, Z.X., Bogdanova, S.V., Collins, A., Davidson, A., De Waele, B., Ernst, R.E.,
875 Fitzsimons, I., Fuck, R., Gladkochub, D., Jacobs, J., Karlstrom, K., Lu, S., Milesi, J-P.,
876 Myers, J., Natapov, L., Pandit, M., Pease, V., Pisarevsky, S.A., Thrane, K., Vernikovsky, V.,
877 2008a. Assembly, configuration, and break-up history of Rodinia: a synthesis. *Precambrian*
878 *Research* 160, 179-210.

879 Li, Z.X., Li, X.H., Li, W.X., Ding, S.J., 2008b. Was Cathaysia part of Proterozoic
880 Laurentia? New data from Hainan Island, south China. *Terra Nova* 20, 154–164.

881 Lubnina N.V., Pisarevsky S.A., Söderlund U., Nilsson M., Sokolov S.J., Khramov A.N.,
882 Iosifidi A.G., Ernst R., Romanovskaya M.A., Pisakin B.N., 2012. New palaeomagnetic and
883 geochronological data from the Roprukey sill (Karelia, Russia): implications for late
884 Palaeoproterozoic palaeogeography. In: Mertanen, S., Pesonen, L. J. and Sangchan, P. (eds.),
885 2012. Supercontinent Symposium 2012 – Programme and Abstracts. Geological Survey of
886 Finland, Espoo, Finland, 81-82.

887 Marcussen, C., Abrahamsen, N., 1983. Palaeomagnetism of the Proterozoic Zig-Zag Dal
888 Basalt and the Midsommerso dolerites, eastern North Greenland. *Geophysical Journal of the*
889 *Royal Astronomic Society* 73, 367-387.

890 Mayer, A., Hofmann, A.W., Sinigoi, S., Morais, E., 2004. Mesoproterozoic Sm-Nd and U-
891 Pb ages for the Kunene Anorthosite Complex of SW Angola. *Precambrian Research* 133,
892 187-206.

893 McCabe, C., Van der Voo, R., 1983. Paleomagnetic results from the upper Keweenawan
894 Chequamegon Sandstone: implications for red bed diagenesis and Late Precambrian apparent
895 polar wander of North America. *Canadian Journal of Earth Sciences* 20, 105-112.

896 McCourt, S., Armstrong, R.A., Kampunzu, A.B., Mapeo, R.B., Morais, E., 2004. New U–
897 Pb SHRIMP ages on zircons from the Lubango region, Southwest Angola: insights into the
898 Proterozoic evolution of South-Western Africa. *Geoscience Africa 2004 (Symposium: The*
899 *birth and growth of continents – geodynamics through time) (Abstract).*

900 Medig, K.P.R., Thorkelson, D.J., Dunlop, R.L., 2010. The Proterozoic Pinguicula Group:
901 Stratigraphy, contact relationships and possible correlations. In: *Yukon Exploration and*
902 *Geology 2009*, MacFarlane, K.E., Weston, L.H., Blackburn, L.R. (eds.), Yukon Geological
903 Survey, 265-278.

904 Meert, J. G., 2002. Paleomagnetic evidence for a Paleo-Mesoproterozoic Supercontinent
905 Columbia. *Gondwana Res.* 5, 207–215.

906 Meert, J.G., Stuckey, W., 2002 Revisiting the paleomagnetism of the 1.476 Ga St.Francois
907 Mountains igneous province, Missouri, *Tectonics* 21,1007, doi:10.1029/2000TC001265.

908 Meert, J.G., Hargraves, R.B., Van der Voo, R., Hall, C.M., Halliday, A.N., 1994.
909 Paleomagnetic and $^{40}\text{Ar}/^{39}\text{Ar}$ studies of Late Kibaran intrusive in Burundi, East Africa:
910 implications for Late Proterozoic supercontinents. *J. Geol.* 102, 621-637.

911 Meert, J.G., Pandit, M.K., Pradhan, V.R., Banks, J., Sirianni, R., Stroud, M., Newstead,
912 B., Gifford, J., 2010. Precambrian crustal evolution of Peninsular India: 3.0 billion year
913 odyssey. *J. Asian Earth Sci.* 39, 483-515.

914 Mertanen, S., Pesonen, L.J., 1995. Paleomagnetic and rock magnetic investigations of the
915 Sipoo Subjotnian quartz porphyry and diabase dykes, southern Fennoscandia. *Phys. Earth*
916 *Planet. Interiors* 88, 145-175.

917 Mertanen, S., Pesonen, L.J., Huhma, H., 1996. Palaeomagnetism and Sm-Nd ages of the
918 Neoproterozoic dykes in Laanila and Kautokeno, northern Fennoscandia. *Geol. Soc. London*
919 *Spec. Publ.* 112, 331-358.

920 Mitchelmore, M.D., Cook, F.A., 1994. Inversion of the Proterozoic Wernicke basin during
921 tectonic development of the Racklan Orogen, northwest Canada. *Can. J. Earth Sci.* 31, 447-
922 457.

923 Mohanty, S., 2010. Tectonic evolution of the Satpura Mountain Belt: a critical evaluation
924 and implication on supercontinent assembly. *J. Asian Earth Sci.* 39, 516-526.

925 Moakhar, M.O., Elming, S.-Å., 2000. A palaeomagnetic analysis of Rapakivi intrusions
926 and related dykes in the Fennoscandian shield. *Phys. Chem. Earth (A)* 25, 5, 489-494.

927 Moores, E.M., 1991. Southwest US – East Antarctic (SWEAT) connection: a hypothesis.
928 *Geology* 19, 425-428.

929 Murthy, G.S., 1978. Paleomagnetic results from the Nain anorthosite and their tectonic
930 implications. *Canad. J. Earth Sci.* 15, 516-525.

931 Myers, J.S., Shaw, R.D., Tyler, I.M., 1996. Tectonic evolution of Proterozoic Australia.
932 *Tectonics* 15(6), 1431-1446.

933 Neuvonen, K.J., 1986. On the direction of remanent magnetization of the quartz porphyry
934 dikes in SE Finland. *Bull. Geol. Soc. Finland* 58, 195-201.

935 Nikishin, A. M., Ziegler, P. A., Stephenson, R. A., Cloetingh, S. A. P. L., Furne, A. V.,
936 Fokin, P. A., Arshov, A. V., Bolotov, S. N., Korotaev, M. V., Alekseev, A. S., Gorbachev, V.
937 I., Shipilov, E. V., Lankreijer, A., Bembinova, E. Yu., Shalimov, I.V. 1996. Late Precambrian
938 to Triassic history of the East European Craton: dynamics of sedimentary basin evolution.
939 *Tectonophysics* 268, 23–63.

940 Onstott, T.C., Hargraves, R.B., York, D., 1984. Dating of Precambrian diabase dikes of
941 Venezuela using paleomagnetic and $^{40}\text{Ar}/^{39}\text{Ar}$ methods. *Anais II Symposium Amazônico*, 2.
942 DNPM, Manaus, Brasil, 513–518.

943 Ovchinnikova, G.V., Semikhatov, M.A., Vasil'eva, I.M., Gorokhov, I.M., Kaurova, O.K.,
944 Podkovyrov, V.N., Gorokhovskii, B.M., 2001. Pb–Pb age of limestones of the middle

945 Riphean Malgina Formation, the Uchur –Maya region of East Siberia. Stratigraphy and
946 Geological Correlation 9, 490–502.

947 Palmer, H.C., Merz, B.A., Hayatsu, A., 1977. The Sudbury dikes of the Grenville Front
948 region: paleomagnetism, petrochemistry, and K-Ar age studies. *Canad. J. Earth Sci.* 14, 1867-
949 1887.

950 Park, J.K., Irving, E., Donaldson, J.A., 1973. Paleomagnetism of the Dubawnt Group.
951 *GSA Bulletin* 84, 859-870.

952 Park, R.G., 1992. Plate kinematic history of Baltica during the Middle to Late Proterozoic:
953 a model. *Geology* 20, 725-728.

954 Pavlov, V.E., Bachtadse, V., Mikhailov, V., 2008. New Middle Cambrian and Middle
955 Ordovician palaeomagnetic data from Siberia: Llandelian magnetostratigraphy and relative
956 rotation between the Aldan and Anabar–Angara blocks. *Earth and Planetary Science Letters*
957 276, 229–242.

958 Pavlov, V.E., Gallet, Y., Shatsillo, A.V., 2000. Palaeomagnetism of the upper Riphean
959 Lakhanda Group of the Uchur–Maya area and the hypothesis of the late Proterozoic
960 supercontinent. *Fizika Zemli* 8, 23– 34 (in Russian).

961 Pavlov, V.E., Gallet, Y., Petrov, P.Yu., Zhuravlev, D.Z., Shatsillo, A.V., 2002. Uy series
962 and late Riphean sills of the Uchur –Maya area: isotopic and palaeomagnetic data and the
963 problem of the Rodinia supercontinent. *Geotectonics* 36, 278– 292.

964 Pesonen, L.J., Neuvonen, K.J., 1981. Palaeomagnetism of the Baltic Shield – implications
965 for Precambrian tectonics. In: Kroner, A. (ed), *Precambrian Plate Tectonics*. Elsevier, 623-
966 648.

967 Pesonen, L. J., Elming, S.-Å., Mertanen, S., Pisarevsky, S. A., D’Agrella-Filho, M. S.,
968 Meert, J. G., Schmidt, P. W., Abrahamsen, N., and Bylund, G., 2003. Palaeomagnetic
969 configuration of continents during the Proterozoic. *Tectonophysics* 375, 289–324.

970 Piper, J.D.A., 1974. Magnetic properties of the Cunene Anorthosite Complex, Angola.
971 *Physics of the Earth and Planetary Interiors* 9, 353-363.

972 Piper, J.D.A., 1979. Palaeomagnetism of the Ragunda intrusion and dolerite dykes,
973 central Sweden. *Geol. Fören. Stockholm Förh.* 101, 139-148.

974 Piper, J.D.A., 1992. The palaeomagnetism of major (Middle Proterozoic) igneous
975 complexes, South Greenland and the Gardar apparent polar wander track. *Precambrian*
976 *Research* 54, 153-172.

977 Piper, J.D.A., Stearn, J.E.F., 1977. Palaeomagnetism of the dyke swarms of the Gardar
978 Igneous Province, South Greenland. *Phys. Earth Planet. Inter.* 14, 345-358.

979 Pisarevsky, S.A., Bylund, G., 2010. Paleomagnetism of 1780-1770 Ma mafic and
980 composite intrusions of Småland (Sweden): implications for the Mesoproterozoic
981 supercontinent. *American Journal of Science* 310, 1168-1186.

982 Pisarevsky, S.A., Sokolov, S.J., 2001. The magnetostratigraphy and a 1780 Ma
983 palaeomagnetic pole from the red sandstones of the Vazhinka River section, Karelia, Russia.
984 *Geophysical Journal International*, 146, 531-538.

985 Pisarevsky, S.A., Natapov, L.M., 2003. Siberia and Rodinia. *Tectonophysics* 375, 221-
986 245.

987 Pisarevsky, S.A., Biswal, T.K., Wang, X-C., De Waele, B., Ernst, R., Söderlund, U., Tait,
988 J.A., Ratre, K., Singh, Y.K., Cleve, M., in press. Palaeomagnetic, geochronological and
989 geochemical study of Mesoproterozoic Lakhna Dykes in the Bastar Craton, India:
990 Implications for the Mesoproterozoic supercontinent. *Lithos*.

991 Pisarevsky, S.A., Wingate, M.T.D., Harris, L.B., 2003a. Late Mesoproterozoic (ca 1.2 Ga)
992 palaeomagnetism of the Albany-Fraser orogen: no pre-Rodinia Australia-Laurentia
993 connection. *Geophysical Journal International* 155, F6-F11.

994 Pisarevsky, S.A., Wingate, M.T.D., Powell, C.McA., Johnson, S., Evans, D.A.D., 2003b.
995 Models of Rodinia assembly and fragmentation. In: Yoshida, M., Windley, B., Dasgupta, S.
996 (eds). Proterozoic East Gondwana: supercontinent assembly and breakup. Geological Society
997 of London Special Publication No 206, 35-55.

998 Pisarevsky, S.A., Natapov, L.M., Donskaya, T.V., Gladkochub, D.P., Vernikovsky, V.A.,
999 2008. Proterozoic Siberia: a promontory of Rodinia. *Precambrian Research* 160, 66–76.

1000 Poprawa, P., Paczeńska, J., 2002. Late Neoproterozoic to Early Palaeozoic development of
1001 a rift at the Lublin-Podlasie slope of the East European Craton – analysis of subsidence and
1002 facies record (eastern Poland). *Przegląd Geologiczny* 50(1), 49-63 (in Polish).

1003 Powell, C.McA., Pisarevsky, S.A., 2002. Late Neoproterozoic assembly of East
1004 Gondwanaland. *Geology* 30, 3-6.

1005 Pradhan, V.R., Pandit, M.K., Meert, J.G., 2008. A cautionary note of the age of the
1006 paleomagnetic pole obtained from the Harohalli dyke swarms, Dharwar craton, southern
1007 India. In: Srivastava, R.K., Sivaji, Ch., Chalapati Rao, N.V. (Eds.), *Indian Dykes:
1008 Geochemistry, Geophysics, and Geochronology*. Narosa Publishing Ltd., New Delhi, India,
1009 pp. 339–352.

1010 Pradhan, V.R., Meert, J.G., Pandit, M.K., Kamenov, G., Gregory, L.C., Malone, 2010.
1011 India's changing place in global Proterozoic reconstructions: new geochronologic constraints
1012 on key paleomagnetic poles from the Dharwar and Aravalli/Bundelkhand Cratons. *Journal of
1013 Geodynamics* 50, 224-242.

1014 Pradhan, V.R., Meert, J.G., Pandit, M.K., Kamenov, G., Mondal, M.E.A., 2012.
1015 Paleomagnetic and geochronological studies of the mafic dyke swarms of Bundelkhand
1016 craton, central India: implications for the tectonic evolution and paleogeographic
1017 reconstructions. *Precambrian Research* 198-199, 51-76.

1018 Reis, N.J., Teixeira, W., Hamilton, M.A., Bispo-Santos, F., Almeida, M.E., D'Agrella-
1019 Filho, M.S., in press. Avanavero mafic magmatism, a late Paleoproterozoic lip in the Guiana
1020 Shield, Amazonian Craton: U–Pb ID-TIMS baddeleyite, geochemical and paleomagnetic
1021 evidence. *Lithos*.

1022 Rivers, T., 1997. Lithotectonic elements of the Grenville Province: review and tectonic
1023 implications. *Precambrian Res.* 86, 117–154.

1024 Ross, G.M., Villeneuve, M.E., Theriault, R.J., 2001. Isotopic provenance of the lower
1025 Muskwa assemblage (Mesoproterozoic, Rocky Mountains, British Columbia): new clues to
1026 correlation and source areas. *Precambrian Research* 111, 57-77.

1027 Roy, J.L., Robertson, W.A., 1978. Paleomagnetism of the Jacobsville Formation and the
1028 apparent polar path for the interval ~1100 to ~670 m.y. for North America. *Journal of*
1029 *Geophysical Research* 83, 1289-1304.

1030 Salminen, J., Pesonen, L. J., 2007. Paleomagnetic and rock magnetic study of the
1031 Mesoproterozoic sill, Valaam island, Russian Karelia: *Precambrian Res.* 159, 212–230.

1032 Salminen, J., Pesonen, L.J., Mertanen, S., Vuollo, J., 2009. Palaeomagnetism of the Salla
1033 Diabase Dyke, northeastern Finland and its implication to the Baltica - Laurentia entity
1034 during the Mesoproterozoic. *Geol. Soc. London Sp. Pub.* 323

1035 Shchipansky, A.A., Bogdanova, S.V., 1996. The Sarmatian crustal segment: Precambrian
1036 correlation between the Voronezh Massif and the Ukrainian Shield across the Dniepr-Donets
1037 aulocogen. *Tectonophysics* 268, 109-125.

1038 Shchipansky, A.A., Samsonov, A.V., Petrova, A.Y., Larionova, Y.O., 2007. Geodynamics
1039 of the Eastern Margin of Sarmatia in the Paleoproterozoic. *Geotectonics* 41 (1), 38–62.

1040 Schmidt, P.W., Williams, G.E., Camacho, A., Lee, J.K.W., 2006. Assembly of Proterozoic
1041 Australia: Implications of a revised pole for the similar to 1070 Ma Alcurra Dyke Swarm,
1042 central Australia. *Geophysical Journal International* 167, 626–634.

1043 Schmidt, P.W., Williams, G.E., 2008. Palaeomagnetism of red beds from the Kimberley
1044 Group, Western Australia: Implications for the palaeogeography of the 1.8Ga King Leopold
1045 glaciations. *Precambrian Research* 167, 267–280.

1046 Schofield, D.I., Thomas, R.J., Goodenough, K.M., De Waele, B., Pitfield, P.E.J., Key,
1047 R.M., Bauer, W., Walsh, G.J., Lidke, D.J., Ralison, A.V., Rabarimanana, M., Rafahatelo,
1048 J.M., Randriamananjara, T., 2010. Geological evolution of the Antongil Craton, NE
1049 Madagascar. *Precambrian Res.* 182, 187-203.

1050 Shcherbakova, V.V., Lubnina, N.V., Shcherbakov, V.P., Mertanen, S., Zhidkov, G.V.,
1051 Vasilieva, T.I., Tsel'movich, V.A., 2008. Palaeointensity and palaeodirectional studies of
1052 early Riphean dyke complexes in the Lake Ladoga region (Northwestern Russia). *Geophys. J.*
1053 *Int.* 175, 433-448.

1054 Snyder, D.B., Lucas, S.B., McBride, J.H., 1996. Crustal and mantle reflectors from
1055 Palaeoproterozoic orogens and their relation to arc-continent collisions. In: Brewer, T.S. (ed),
1056 *Precambrian crustal evolution in the North Atlantic Region. Geological Society Special*
1057 *Publication* 112, 1-23.

1058 Söderlund, U., Isachsen, C.E., Bylund, G., Heaman, L., Patchett, P.J., Vervoort, J.D.,
1059 Andersson, U.B., 2005. U-Pb baddeleyite ages and Hf, Nd isotope chemistry constraining
1060 repeated mafic magmatism in the Fennoscandian Shield from 1.6 to 0.9 Ga. *Contrib. Mineral.*
1061 *Petr.* 150, 174-194.

1062 Srivastava, R.K., Singh, R.K., Verma, S.P., 2004. Neoproterozoic mafic volcanic rocks from
1063 the southern Bastar greenstone belt, Central India: petrological and tectonic significance.
1064 *Precambrian Res.* 131, 305-322.

1065 Starmer, I.C., 1996. Accretion, rifting and collision in the North Atlantic supercontinent,
1066 1700 – 950 Ma. In: Brewer, T.S. (ed), *Precambrian Crustal Evolution in the North Atlantic*
1067 *region, Geological Society of London Special Publication* 112, 219-248.

1068 Tack, L., Wingate, M.T.D. De Waele, B, Meert, J., Belousova, E., Griffin, B., Tahon, A.,
1069 Fernandez-Alonso, M., 2010. The 1375Ma “Kibaran event” in Central Africa: Prominent
1070 emplacement of bimodal magmatism under extensional regime. *Precambrian Research* 180,
1071 63–84, doi:10.1016/j.precamres.2010.02.022.

1072 Teixeira, W., Sabate, P., Barbosa, J., Noce, C.M., Carneiro, M.A., 2000. Archean and
1073 Paleoproterozoic tectonic evolution of the São Francisco craton, Brazil. In: Cordiani, U.G.,
1074 Milani, E.J., Thomaz Filho, A., Campos, D.A.(eds), *Tectonic evolution of South America*,
1075 Rio de Janeiro, pp.101-137.

1076 Thorkelson, D.J., Abbott, J.G., Mortensen, J.K., Creaser, R.A., Villeneuve, M.E.,
1077 McNicoll, V.J., Layer, P.W., 2005. Early and Middle Proterozoic evolution of Yukon,
1078 Canada. *Canadian Journal of Earth Sciences* 42(6), 1045-1071.

1079 Tohver, E., Van Der Pluijm, B.A., Van Der Voo, R., Rizzotto, G., Scandolara, J.E., 2002.
1080 Paleogeography of the Amazon craton at 1.2 Ga: Early Grenvillian collision with the Llano
1081 segment of Laurentia, *Earth planet. Sci. Lett.* 199, 185–200.

1082 Trompette, R., 1994. *Geology of Western Gondwana (2000 – 500 Ma)*. A.A. Balkema,
1083 Rotterdam/Brookfield, 350 p.

1084 Tucker, R.D., Ashwal, L.D., Torsvik, T.H., 2001. U-Pb geochronology of Seychelles
1085 granitoids: a Neoproterozoic continental arc fragment. *Earth. Planet. Sci. Lett.* 187, 27-38.

1086 Veikkolainen, T., Pesonen, L.J., Kohronen, K., Evans, D.A.D., 2012. The Precambrian
1087 geomagnetic field has no prominent low-inclination bias. In: Mertanen, S., Pesonen, L.J.,
1088 Sangchan, P., *Supercontinent Symposium 2012 – Programme and Abstracts*. Geological
1089 Survey of Finland, Espoo, Finland, p. 151-152.

1090 Veselovsky, R.V., Petrov, P.Yu., Karpenko, S.F., Kostitsyn, Yu.A., Pavlov, V.E., 2006.
1091 New paleomagnetic and isotopic data from the Late Proterozoic magmatic complex of the
1092 northern slope of the Anabar uplift. *Doklady Akad.Nauk Rossii* 410, 1-6 (in Russian).

1093 Vodovozov, V.Yu., Didenko, A.N., Gladkochub, D.P., Mazukabzov, A.M., Donskaya,
1094 T.V., 2007. Paleomagnetic results from the Early Proterozoic rocks of the Baikal Inlet of the
1095 Siberian Craton. *Fizika Zemli* 10, 60-72 (in Russian).

1096 Warnock, A.C., Kodama, K.P., Zeitler, P.K., 2000. Using thermochronometry and low-
1097 temperature demagnetization to accurately date Precambrian paleomagnetic poles. *Journal of*
1098 *Geophysical Research* 105, 19435–19453.

1099 Williams, G.E., Schmidt, P.W., Clark, D.A., 2004. Palaeomagnetism of iron-formation
1100 from the late Palaeoproterozoic Frere Formation, Earaheedy Basin, Western Australia:
1101 palaeogeographic and tectonic implications. *Precambrian Research* 128, 367-383.

1102 Wingate, M. T. D., Pisarevsky, S. A., Evans, D. A. D., 2002. A revised Rodinia
1103 supercontinent: no SWEAT, no AUSWUS. *Terra Nova* 14, 121-128.

1104 Wingate, M.T.D., Pisarevsky, S.A., Gladkochub, D.P., Donskaya, T.V., Konstantinov,
1105 K.M., Mazukabzov, A.M., Stanevich, A.M., 2009. Geochronology and paleomagnetism of
1106 mafic igneous rocks in the Olenek Uplift, northern Siberia: implications for Mesoproterozoic
1107 supercontinents and paleogeography. *Precambrian Research* 170, 256-266.

1108 Winston, D., Link, P.K., 1993. Middle Proterozoic rocks of Montana, Idaho and
1109 eastern Washington: the Belt Supergroup. In: Reed Jr., J.C., Bickford, M.E., Houston, R.S.,
1110 Link, P.K., Rankin, D.W., Sims, P.K., Van Schmus, W.R. (Eds.), *Precambrian:*
1111 *Conterminous US Geol. Soc. Am., The Geology of North America C-2*, pp. 487–517.

1112 Wu, H.C., Zhang, S.H., Li, Z.X., Li, H.Y., Dong, J., 2005. New paleomagnetic results
1113 from the Yangzhuang Formation of the Jixian System, North China, and tectonic
1114 implications. *Chinese Science Bulletin* 50, 1483-1489.

1115 Zhang, S., Li, Z.X., Evans, D.A.D., Wu, H., Li, H., Dong, J., 2012. Pre-Rodinia
1116 supercontinent Nuna shaping up: A global synthesis with new paleomagnetic results from
1117 North China. *Earth and Planetary Science Letters* 353-354, 145-155.

- 1118 Zhao, G.C., 2009. Metamorphic evolution of major tectonic units in the basement of the
1119 North China Craton: Key issues and discussion. *Acta Petrologica Sinica* 25, 1772–1792.
- 1120 Zhao, G.C., Cawood, P.A., 2012. Precambrian geology of China. *Precambrian Research*
1121 222-223, 13-54.
- 1122 Zhao, G.C., Cawood, P.A., Wilde, S.A., Sun, M., 2002. A review of the global 2.1–1.8 Ga
1123 orogens: implications for a pre-Rodinian supercontinent. *Earth Sci. Rev.* 59, 125-162.
- 1124 Zhao, G.C., Sun, M., Wilde, S.A., Li, S.Z., 2004. A Paleo-Mesoproterozoic
1125 supercontinent: Assembly, growth and breakup. *Earth Sci. Rev.* 67, 91-123.
- 1126

1 **Figure captions**

2 **Fig. 1** Time-space distribution of late Paleoproterozoic and Mesoproterozoic paleomagnetic
3 data for different cratons.

4 **Fig. 2.** Laurentia-Baltica reconstruction (a) and Laurentian and Baltican paleopoles for the
5 time interval 1800 – 1270 Ma plotted in Laurentian coordinates. Baltica is rotated to
6 Laurentia about a pole at 44.99°N, 7.45°E by +44.93°.

7 **Fig. 3.** Paleomagnetically supported reconstruction of Siberia and Laurentia at ca. 1000 Ma.
8 Laurentia is rotated to the absolute framework about a pole at 24.21°N, 175.26°E by -
9 150.19°. Siberia is rotated to Laurentia about a pole at 69.95°N, 133.23°E by +127.05°.

10 Internal rotations in Siberia are also applied (see Section 3). Paleopoles' numbers are as in
11 Table 1.

12 **Fig. 4.** Baltica – Amazonia SAMBA reconstruction, simplified from Johansson (2009).

13 **Fig. 5.** Paleomagnetic test of the SAMBA reconstruction: (a-c) at 1790 Ma; (d-f) at 1420 Ma.
14 See text in Section 6.

15 **Fig. 6.** Geological matches in the paleomagnetically permissive Baltica-India reconstruction
16 (after Pisarevsky et al., in press). India is rotated to Baltica about a pole at 30.7°N, 54.3°E by
17 -184.9°.

18 **Fig. 7.** Global paleogeographic reconstruction at 1770 Ma. Filled polygons represent Archean
19 crust. Paleopoles' numbers are as in Table 1 on the polar projection. La=Laurentia,
20 Fennosc=Fennoscandia, VU=Volgo-Uralia, Sar=Sarmatia, NAC=North Australian craton,
21 WAC=West Australian Craton, SAC=South Australian Craton, Maw=Mawson Craton,
22 Si=Siberia, SF= São Francisco, Kal=Kalahari, Am=Amazonia, WA=West Africa, NC=North
23 China.

24 **Fig. 8.** Global paleogeographic reconstruction at 1720 Ma. See notes to Fig. 7.

25 **Fig. 9.** Global paleogeographic reconstruction at 1650 Ma. Ba=Baltica. See notes to Fig. 7.

26 **Fig. 10.** Global paleogeographic reconstruction at 1580 Ma. The star denotes the position of
27 the mantle plume head. See notes to Fig. 7.

28 **Fig. 11.** Global paleogeographic reconstruction at 1500 Ma. See notes to Fig. 7.

29 **Fig. 12.** Global paleogeographic reconstruction at 1470 Ma. See notes to Fig. 7.

30 **Fig. 13.** Global paleogeographic reconstruction at 1540 Ma. See notes to Fig. 7.

31 **Fig. 14.** Global paleogeographic reconstruction at 1380 Ma. See notes to Fig. 7.

32 **Fig. 15.** Global paleogeographic reconstruction at 1270 Ma. See notes to Fig. 7.

33

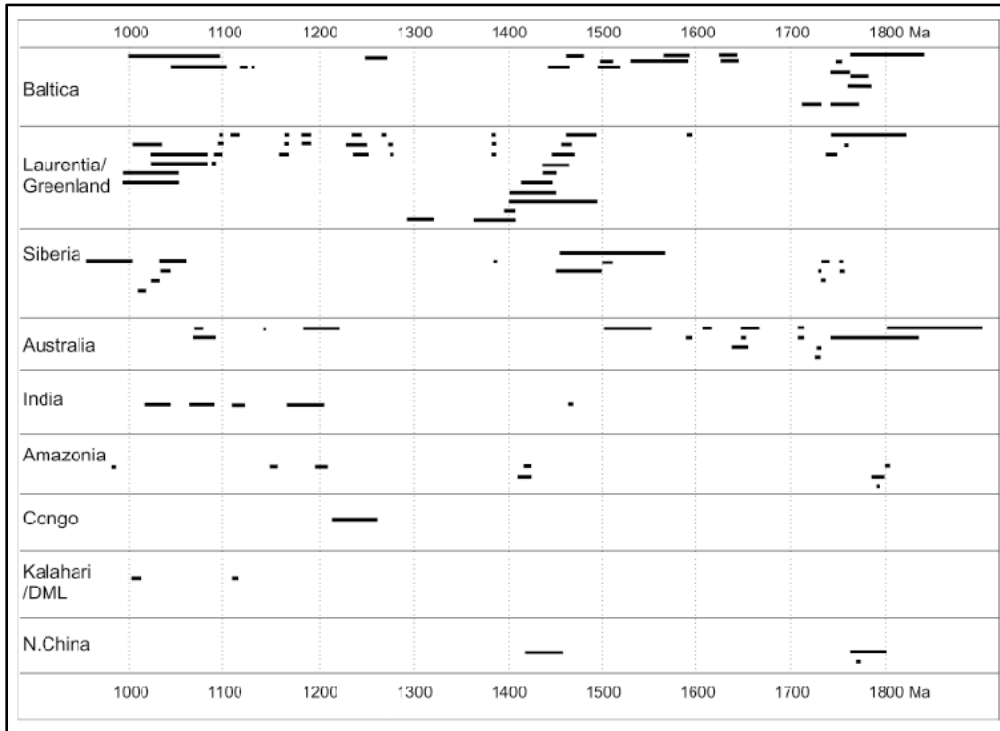


Figure 1

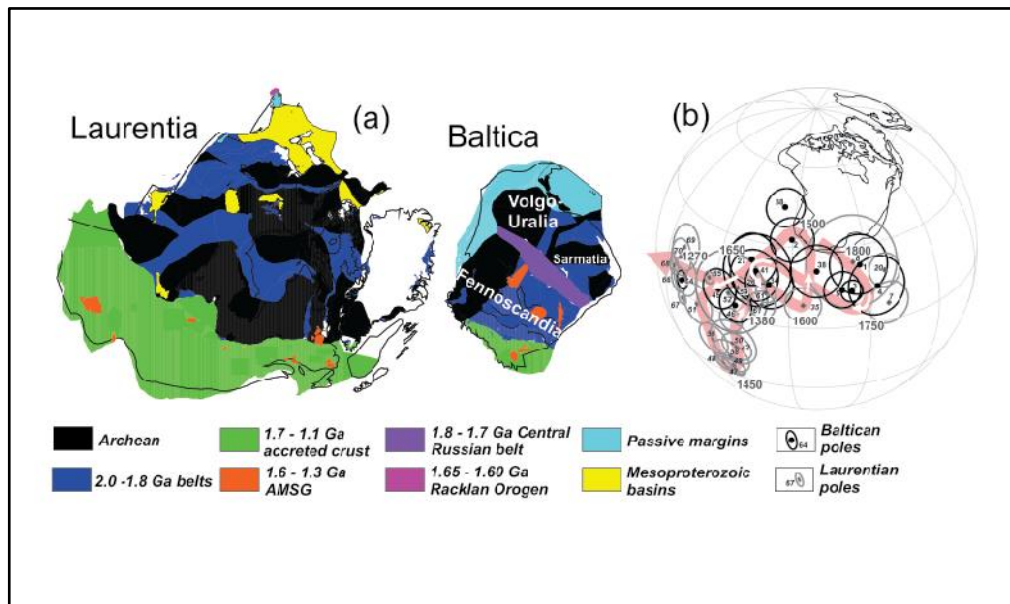


Figure 2

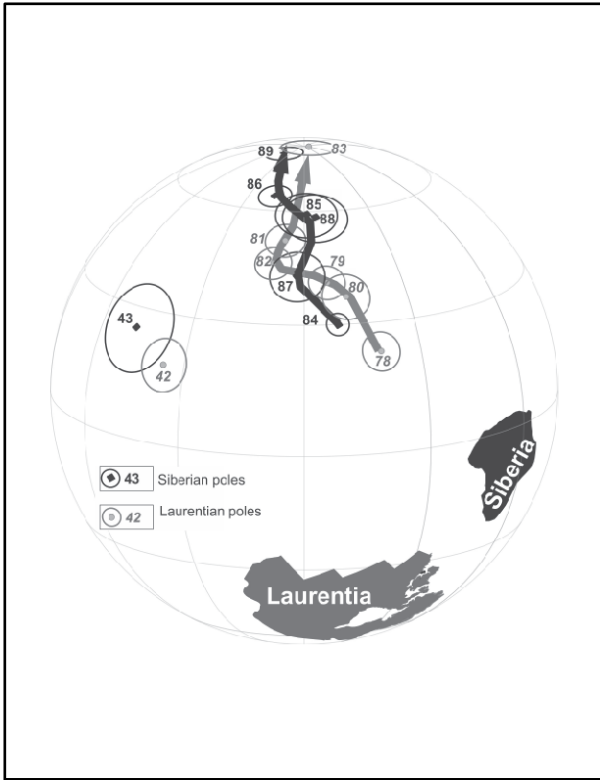


Figure 3

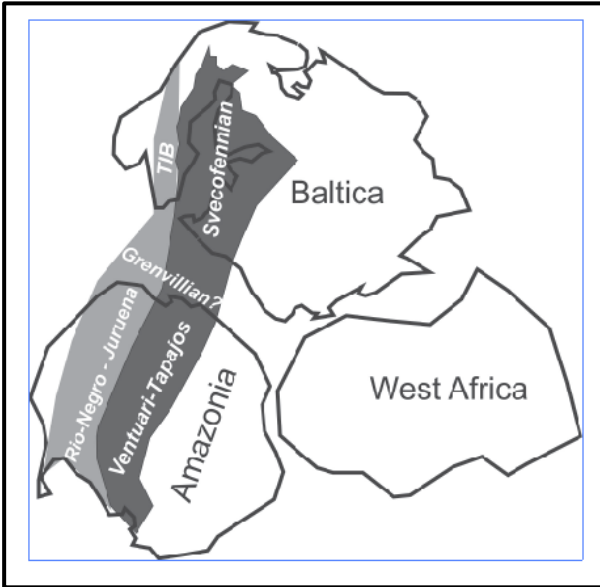


Figure 4

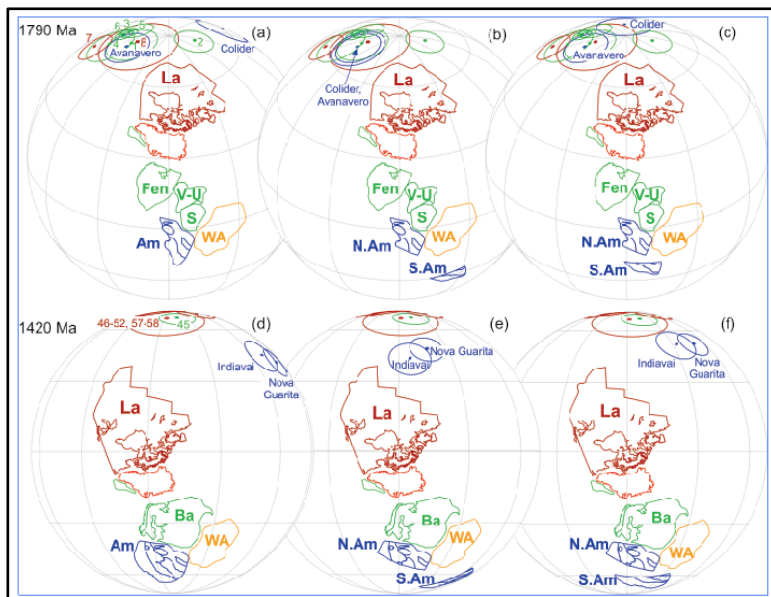


Figure 5

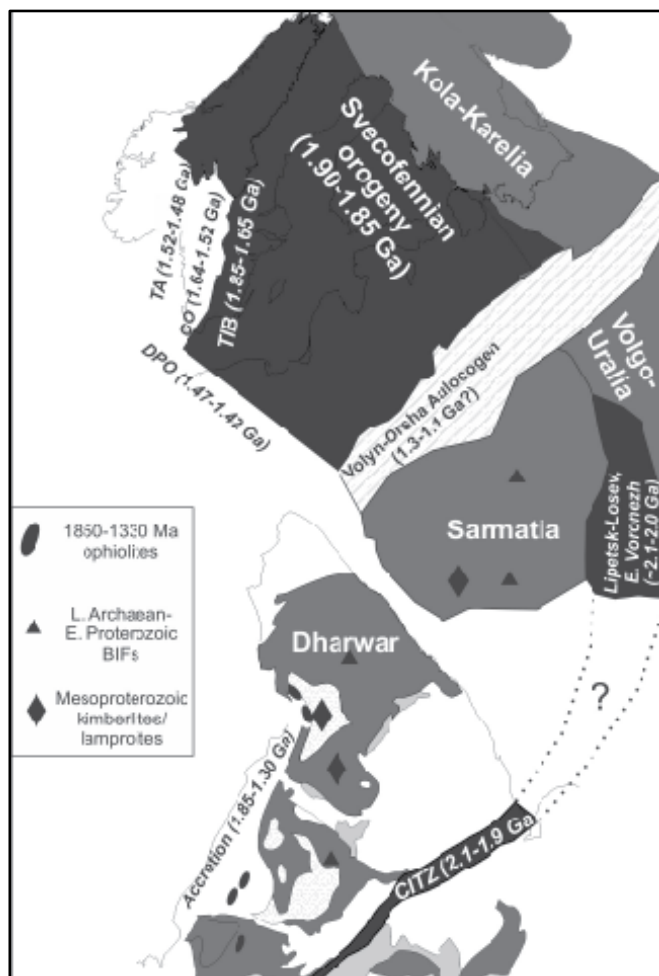


Figure 6

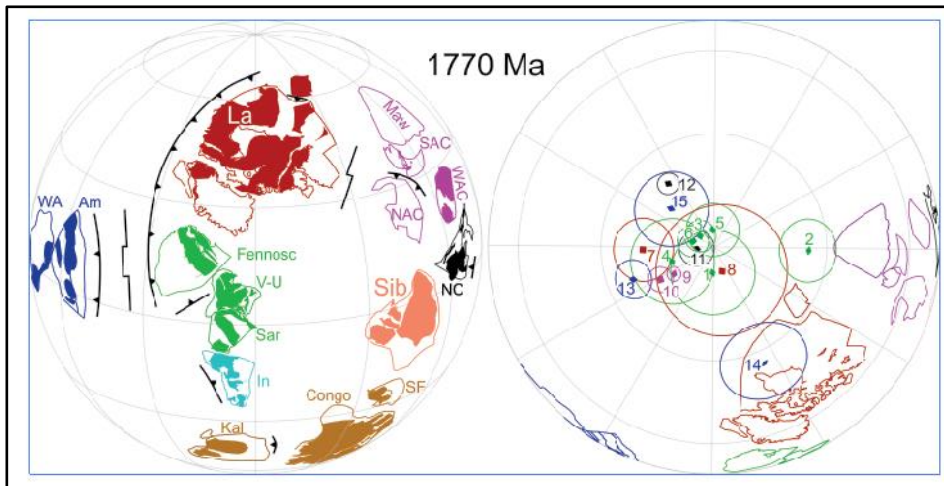


Figure 7

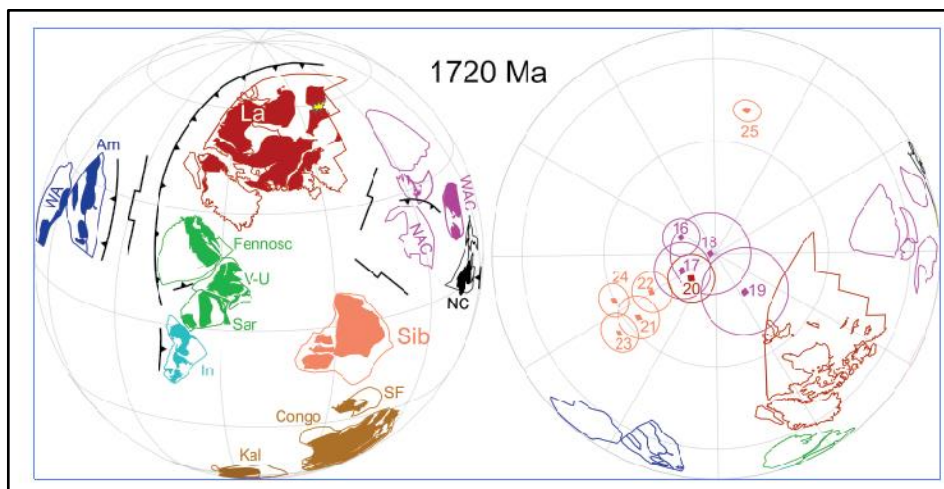


Figure 8

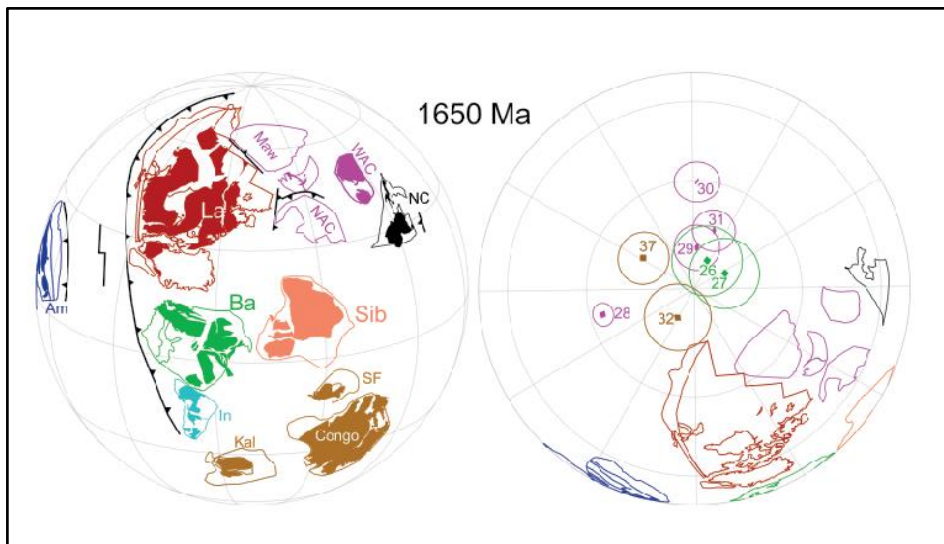


Figure 9

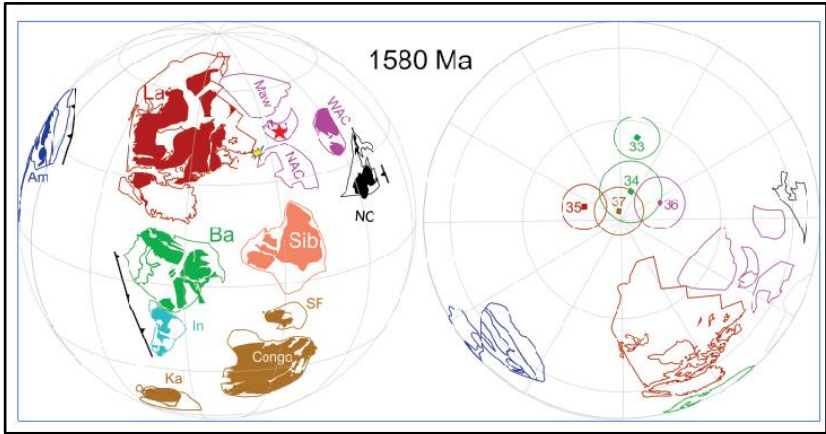


Figure 10

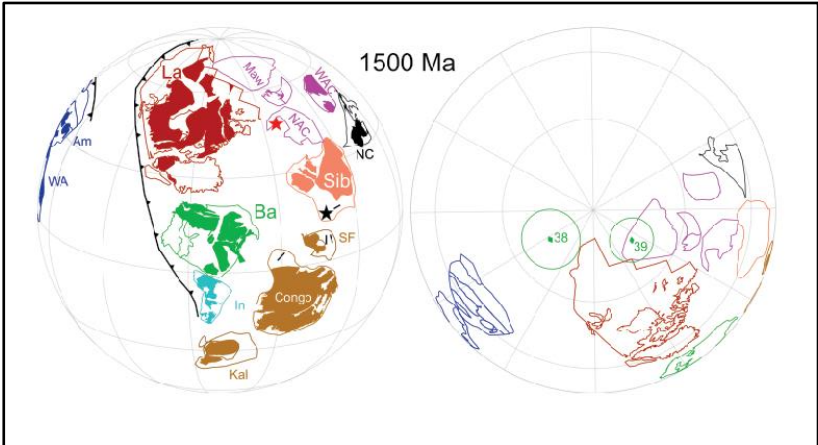


Figure 11

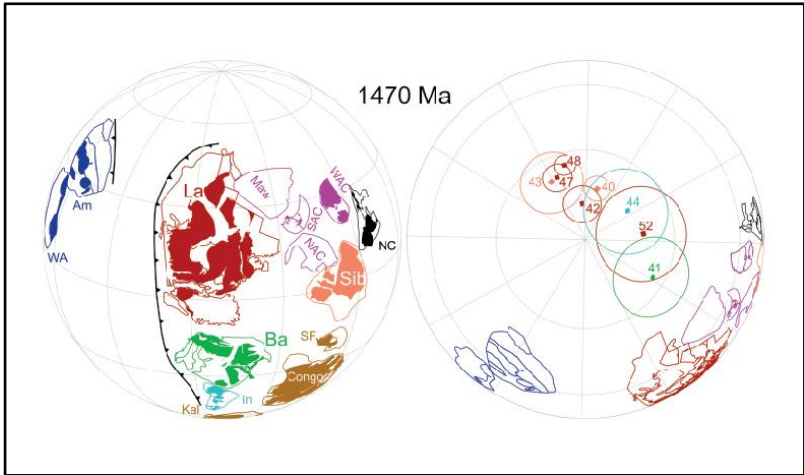


Figure 12

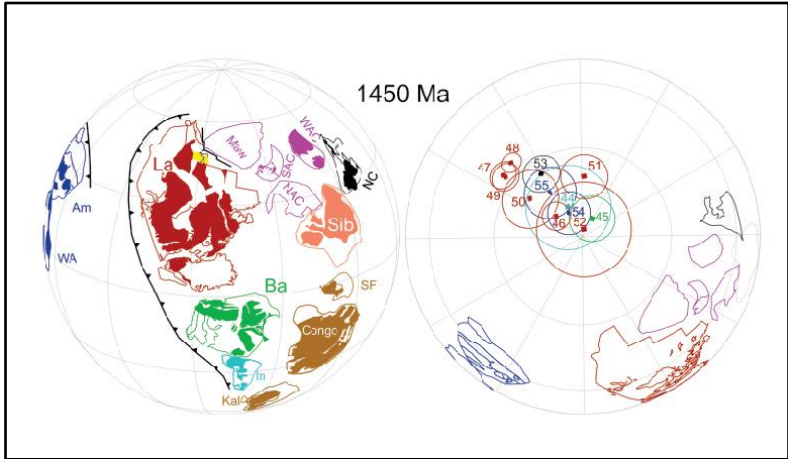


Figure 13

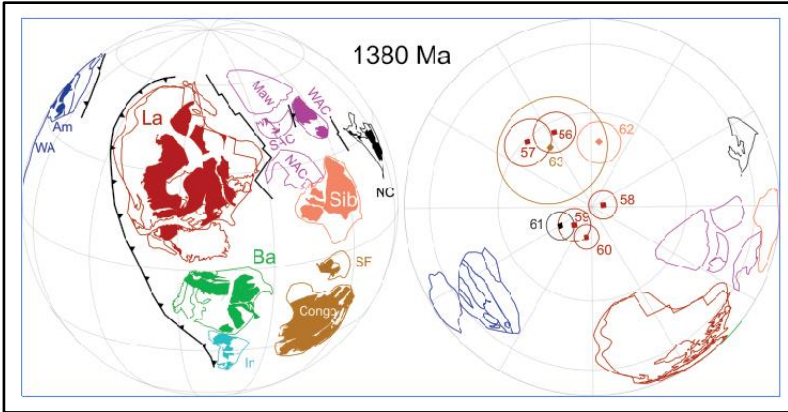


Figure 14

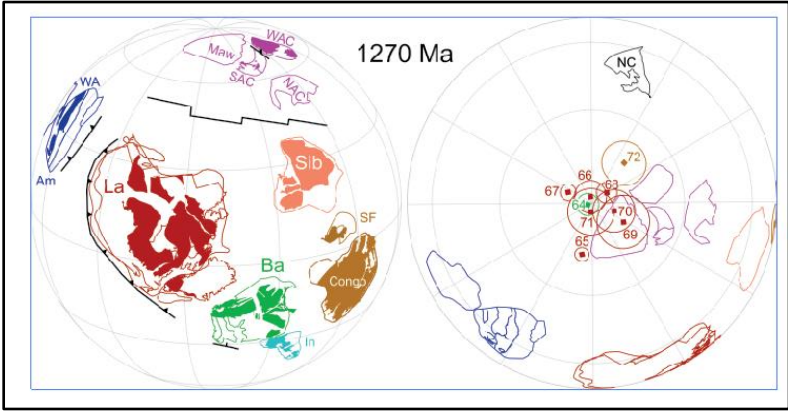


Figure 15

Table 1. Selected 1800-1000 Ma paleomagnetic poles (modified from the Luleå Workshop 2009 compilation).

#	Rockname	Continent	Age (Ma)	Plat (°N)	Plong (°E)	A ₉₅ (°)	Reference
1770 Ma							
1	Late. Svecofennian Rocks, Mean	Fenn	~1800	49.6	221.0	10.8	In: Elming and Pesonen, 2010.
2	Småland Intrusions	Fenn	1784-1769	45.7	182.7	8.0	Pisarevsky and Bylund, 2010
3	Shoksha Formation	Fenn	1780-1760	39.7	221.1	4.0	Pisarevsky and Sokolov, 2001
4	Hoting Gabbro	Fenn	1760-1740	43.0	233.3	10.9	Elming et al., 2009b
5	Roprukey Sill	Fenn	1754-1748	39.1	216.6	6.7	Fedotova et al., 1999; Lubnina et al., 2012
6	Korosten Pluton	Sarm	1770-1740	25.1	171.0	4.0	Elming et al., 2001
7	Dubawnt Group	Lau	1820-1750	7.0	277.0	8.0	Park et al., 1973
8	Jan Lake Granite	Lau	1759-1757	24.3	264.3	16.9	Gala et al., 1995
9	<i>Frere Formation</i>	WAC	<i>1900-1800</i>	<i>45.2</i>	<i>40.0</i>	<i>1.8</i>	<i>Williams et al., 2004</i>
10	<i>Elgee-Pentecost Formations</i>	NAC	<i>1834-1740</i>	<i>5.4</i>	<i>31.8</i>	<i>3.2</i>	<i>Schmidt and Williams, 2008; Wingate et al., 2011</i>
11	Xiong'er Group	N.Chi	~1780	50.2	263.0	4.5	Zhang et al., 2012
12	Taihang Dykes	N.Chi	1772-1766	36.0	247.0	2.8	Halls et al., 2000
13	Basic Dykes Group II	Am	1802-1798	42.0	180.0	5.0	Onstott et al., 1984
14	Colider Volcanics	Am	1796-1782	63.3	118.8	11.4	Bispo-Santos et al., 2008
15	Avanavero Intrusions	Am	1791-1786	48.4	207.9	9.6	Reis et al., in press
1720 Ma							
16	Peters Creek Volc., upper part	NAC	1729-1725	26.0	41.0	4.8	Idnurm, 2000
17	Wollogorang Formation	NAC	1730-1723	17.9	38.2	7.2	Idnurm et al., 1995
18	Fiery Creek Formation	NAC	1712-1706	23.9	31.8	10.4	Idnurm, 2000
19	West Branch Volcanics	NAC	1712-1705	15.9	20.50	11.3	Idnurm, 2000
20	Cleaver Dykes	Lau	1745-1736	19.4	276.7	6.1	Irving et al., 2004
21	<i>Chaya Dyke 1 VGP</i>	<i>Sib</i>	<i>1755-1749</i>	<i>40.0</i>	<i>280.0</i>	<i>5.7</i>	<i>Vodovozov et al., 2007; Gladkochub et al., 2010</i>
22	<i>Chaya Dyke 2 VGP</i>	<i>Sib</i>	<i>1755-1749</i>	<i>39.0</i>	<i>270.0</i>	<i>5.3</i>	<i>Vodovozov et al., 2007; Gladkochub et al., 2010</i>
23	<i>Angara-Kan Granite VGP</i>	<i>Sib</i>	<i>1739-1729</i>	<i>42.9</i>	<i>289.6</i>	<i>5.3</i>	<i>Didenko et al., 2009</i>

24	Ulkan Granite*	Sib	1730-1725	48.0	278.8	4.4	Didenko et al., 2013
25	Elgetei Formation*	Sib	1736-1728	18.1	210.6	3.6	Didenko et al., 2013
1650 Ma							
26	Sipoo Quartz Porphyry Dykes	Ba	1643-1623	26.4	180.4	9.4	Mertanen and Pesonen, 1995
27	Finnish Quartz Porphyry Dykes	Ba	1641-1621	30.2	175.4	9.4	Neuvonen, 1986
28	Mallpunyah Formation	NAC	1665-1645	35.0	34.3	3.1	Idnurm et al., 1995
29	Tooganinie Formation	NAC	1651-1645	61.0	6.7	6.1	Idnurm et al., 1995
30	Emmerugga Dolomite	NAC	1653-1635	79.1	22.6	6.1	Idnurm et al., 1995
31	Balbirini Dolomite, lower part	NAC	1617-1606	66.1	357.5	5.7	Idnurm, 2000
32	<i>Bathlaros Kimberlite</i>	<i>Kal</i>	<i>1700-1600</i>	<i>30.0</i>	<i>8.2</i>	<i>8.9</i>	<i>Hargraves et al., 1989</i>
1580 Ma							
33	Kumlinge-Brändö Dykes	Ba	1590-1562	12.2	182.0	6.7	Pesonen and Neuvonen, 1981
34	Föglö-Sottunga Dykes	Ba	1589-1528	27.8	187.5	9.0	Pesonen and Neuvonen, 1981
35	Western Channel Diabase	Lau	1593-1587	9.0	245.0	6.6	Irving et al., 1972; Hamilton and Buchan, 2010
36	Balbirini Dolomite, upper part	NAC	1592-1586	52.0	356.1	7.5	Idnurm, 2000
37	<i>Van Dyk Mine Dyke.</i>	<i>Kal</i>	<i>1650-1550</i>	<i>12.4</i>	<i>13.9</i>	<i>7.0</i>	<i>Jones and McElhinny, 1966</i>
1500 Ma							
38	Rødø basic dykes	Ba	1513-1497	41.6	201.7	9.5	Moakhar and Elming, 2000
39	Ragunda Formation	Ba	1519-1493	51.6	166.6	7.1	Piper, 1979
1470 Ma							
40	<i>Fomich Mafic Intrusions</i>	<i>Sib</i>	<i>1564-1452</i>	<i>19.2</i>	<i>257.2</i>	<i>4.2</i>	<i>Veselovsky et al., 2006</i>
41	Bunkris/Glysjon/Oje Rocks	Ba	1478-1460	28.3	179.8	13.2	Bylund, 1985; Söderlund et al., 2005
42	St.Francois Mountains	Lau	1492-1460	-13.2	219.0	6.1	Meert and Stuckey, 2002
43	Kyutingde, Sololi intrusions, Siberia	Sib	1497-1449	33.6	253.1	10.4	Wingate et al., 2009
44	Lakhna Dykes, India	Ind	1468-1462	36.6	132.8	14.0	Pisarevsky et al., in press
1450-1420 Ma							
45	Ladoga-Valaam Intrusions	Ba	1464-1440	11.8	173.3	7.4	Salminen and Pesonen, 2007; Shcherbakova et al., 2008

46	Michikamau Intrusion	Lau	1465-1455	-1.5	217.5	4.7	Emslie et al., 1976
47	Spokane Formation	Lau	1470-1445	-24.8	215.5	4.7	Elston et al., 2002
48	Snowslip Formation	Lau	1463-1436	-24.9	210.2	3.5	Elston et al., 2002
49	Purcell Lava	Lau	1450-1436	-23.6	215.6	4.8	Elston et al., 2002
50	Rocky Mountain Intrusions, Mean	Lau	1445-1415	-11.9	217.4	9.7	In: Elming and Pesonen, 2010.
51	Mistastin Pluton	Lau	1450-1400	-1.0	201.5	7.6	Fahrig and Jones, 1976
52	Tobacco Root Dykes A	Lau	1497-1399	8.7	216.1	15.5	Harlan et al., 2008
53	Tieling Formation	N.Chi	1458-1416	11.6	187.1	6.3	Wu et al., 2005
54	Nova Guarita Intrusives	Am	1423-1415	47.9	65.9	7.0	Bispo-Santos et al., 2012
55	Indiavai Intrusion	Am	1423-1409	57.0	69.7	8.6	D'Agrella-Filho et al., 2012
1380 Ma							
56	McNamara Formation	Lau	1407-1395	-13.5	208.3	6.7	Elston et al., 2002
57	Pilcher, Garnet Range, Libby Formations	Lau	1407-1362	-19.2	215.3	7.7	Elston et al., 2002
58	Victoria Fjord Dolerite Dykes	Gre	1384-1380	10.3	231.7	4.3	Abrahamsen and Van der Voo, 1987
59	Midsommersoer Dolerite	Gre	1384-1380	6.9	242.0	5.1	Marcussen and Abrahamsen, 1983
60	Zig-Zag Dal Basalts	Gre	1384-1380	12.0	242.8	3.8	Marcussen and Abrahamsen, 1983
61	N.China Sills	N.Chi	1367-1333	5.9	359.6	4.3	Chen et al., 2013
62	<i>Chieress Dyke VGP</i>	<i>Sib</i>	<i>1386-1382</i>	<i>5.0</i>	<i>258.0</i>	<i>6.7</i>	<i>Ernst et al., 2000</i>
63	<i>Kunene Complex</i>	<i>Con</i>	<i>1385-1375</i>	<i>-3.0</i>	<i>255.0</i>	<i>17.4</i>	<i>Piper, 1974; Mayer et al., 2004; Drüppel et al., 2000; McCourt et al., 2004</i>
1270 Ma							
64	Post-Jotnian Intrusions	Ba	1270-1246	-1.8	159.1	3.4	In: Elming and Pesonen, 2010.
65	Nain Anorthosite	Lau	1320-1290	11.7	206.7	2.2	Murthy, 1978
66	Mackenzie Dykes	Lau	1269-1265	4.0	190.0	5.0	Buchan and Halls (1990), LeCheminant and Heaman (1989)
67	Sudbury Dykes	Lau	1242-1232	-2.5	192.8	2.5	Palmer et al., 1977
68	Kungnat Ring Dyke	Gre	1277-1273	3.4	198.7	3.2	Piper and Stearn, 1977
69	North Qoroq Intrusions	Gre	1276-1274	13.2	202.6	8.3	Piper, 1992
70	West Gardar Dolerite Dykes	Gre	1251-1236	8.7	201.7	6.6	Piper and Stearn, 1977

71	West Gardar Lamprophyre Dykes	Gre	1249-1227	3.2	206.4	7.2	Piper and Stearn, 1977
72	Late Kibaran Intrusions	Con	1260-1212	-17.0	112.7	7.0	Meert et al., 1994
Younger poles							
73	<i>Salla Dyke VGP</i>	<i>Ba</i>	<i>1129-1115</i>	<i>71.0</i>	<i>113.0</i>	<i>8.0</i>	<i>Salminen et al., 2009</i>
74	<i>Bamble Intrusions</i>	<i>Ba</i>	<i>1100-1040</i>	<i>-15.1</i>	<i>222.5</i>	<i>19.3</i>	<i>Lulea, 2009 workshop</i>
75	<i>Laanila Dolerite</i>	<i>Ba</i>	<i>1095-995</i>	<i>-2.1</i>	<i>212.2</i>	<i>13.8</i>	<i>Mertanen et al., 1996</i>
76	Abitibi Dykes	Lau	1143-1139	44.4	211.4	13.7	Ernst and Buchan, 1993
77	Nipigon Sills and Lavas, Mean	Lau	1115-1107	47.2	217.8	4.0	In: Elming and Pesonen, 2010.
78	Lake Shore Traps	Lau	1089-1085	22.2	180.8	4.5	Diehl and Haig, 1994; Davis and Paces, 1990
79	Freda Sandstone	Lau	1080-1020	2.2	179.0	4.2	Henry et al., 1977; Wingate et al., 2002
80	Nonesuch Shale	Lau	1080-1020	7.6	178.1	5.5	Henry et al., 1977; Wingate et al., 2002
81	Chequamegon Sandstone	Lau	1050-990	-12.3	177.7	4.6	McCabe and Van der Voo, 1983
82	Jacobsville Sandstone	Lau	1050-990	-10.0	184.0	4.2	Roy and Robertson, 1978
83	Haliburton Intrusion	Lau	1030-1000	-32.6	141.9	6.3	Warnock et al., 2000
84	Malgina Formation*	Sib	1043±14	-15.4	248.8	2.6	Gallet et al., 2000; Ovchinnikova et al., 2001
85	Kumakha Formation*	Sib	1040-1030	-3.2	221.4	7.0	Pavlov et al., 2000
86	Milkon Formation*	Sib	~1025	5.1	216.3	3.8	Pavlov et al., 2000
87	Nelkan Formation*	Sib	1025-1015	-4.4	238.8	6.3	Pavlov et al., 2000
88	Ignikan Formation*	Sib	1015-1005	-5.3	221.8	7.4	Pavlov et al., 2000
89	Kandyk Formation*	Sib	1000-950	7.0	196.7	4.3	Pavlov et al., 2002
90	W. Australian Rocks, Mean	WAC	1220-1180	59.9	331.8	27.0	Pisarevsky et al., 2003a
93	Harohalli Alkaline Dykes	Ind	1202-1182	24.9	78.0	15.0	Pradhan et al., 2008
94	Mahoba Dykes	Ind	1120-1106	38.7	229.5	12.4	Pradhan et al., 2012
95	<i>Majhgawan Kimberlite VGP</i>	<i>Ind</i>	<i>1088-1060</i>	<i>36.8</i>	<i>212.5</i>	<i>12.2</i>	<i>Gregory et al., 2006</i>
96	Anantapur Dykes	Ind	1040-1014	10.0	211.4	11.0	Pradhan et al., 2010

* Rotated to Anabar at 62°N, 117°E, 23°

Non-key poles are shown in italics

Table 2. Euler rotation parameters (to the absolute framework).

Craton/block/terrane	Pole		Angle
	(°N)	(°E)	(°)
1770 Ma			
Laurentia	-52.03	60.09	215.25
Greenland	-51.30	63.17	228.72
Fennoscandia	-66.33	26.88	199.92
Sarmatia/Volgo-Uralia	-57.98	-10.80	172.80
India	-24.88	132.46	208.11
Wyoming	-53.02	60.69	215.51
NAC	-33.26	-0.68	206.88
WAC	-17.03	9.34	190.76
SAC	-1.92	18.32	177.99
Mawson	3.21	17.57	206.50
North China	-71.97	73.84	191.52
Siberia	-6.45	-0.31	121.40
Congo	-19.10	121.62	122.91
São Francisco	-15.26	97.91	86.64
Kalahari	17.65	116.44	114.65
Dronning Maud Land	-1.68	99.43	71.54
Rockall	-52.19	73.21	233.39
Amazonia	12.24	47.02	-166.35
West Africa	28.68	66.70	179.99
1720 Ma			
Laurentia	-53.49	67.66	212.01
Greenland	-53.24	70.77	225.55
Fennoscandia	-68.38	35.70	194.11
Sarmatia/Volgo-Uralia	-66.51	16.45	183.12
India	-9.21	136.35	202.59
NAC	-31.05	8.72	203.04
WAC	-13.59	17.19	190.00
SAC	2.42	25.32	179.87
Mawson	5.74	25.61	209.45
North China	-68.59	73.42	176.38
Siberia	1.70	-13.68	115.28
Congo	-34.13	118.34	114.92
São Francisco	-33.41	95.14	71.86
Kalahari	-10.81	-59.61	-103.20
Dronning Maud Land	-10.65	103.77	58.09
Rockall	-53.85	81.22	230.04
Amazonia	5.04	49.98	-151.23
West Africa	24.68	67.25	-160.07
1650 Ma			
Laurentia	-55.43	47.53	189.94
Greenland	-54.61	50.11	203.53
Baltica	-61.66	7.18	177.17
India	-16.14	135.69	199.83
NAC	-19.89	-1.91	184.72
WAC	-6.28	8.67	163.66
SAC	6.75	20.09	148.13
Mawson	10.74	22.67	176.97

North China	-71.38	22.13	177.25
Siberia	1.26	-19.76	98.53
Congo	-42.12	122.86	126.97
São Francisco	-45.07	106.43	79.56
Kalahari	-7.68	-58.91	240.38
Dronning Maud Land	-11.98	112.33	72.73
Rockall	-57.30	58.51	209.80
Amazonia	-5.74	41.42	-170.83
West Africa	10.81	60.89	-174.71

1580 Ma

Laurentia	-54.53	52.84	191.84
Greenland	-53.92	55.53	205.45
Baltica	-62.58	13.84	178.40
India	-13.21	136.86	197.48
NAC	-21.56	-0.07	189.25
WAC	-7.17	10.05	169.41
SAC	6.44	20.74	154.59
Mawson	10.43	22.98	183.51
North China	-71.37	32.48	177.56
Siberia	-10.49	-7.62	106.70
Congo	-27.82	121.43	135.59
São Francisco	-28.22	101.60	93.67
Kalahari	7.82	113.30	106.14
Dronning Maud Land	-17.65	97.61	66.07
Rockall	-56.31	64.35	211.21
Amazonia	-13.40	42.34	-155.37
West Africa	6.43	59.46	-155.01

1500 Ma

Laurentia	-59.30	53.77	179.10
Greenland	-58.93	55.76	192.93
Baltica	-64.38	9.28	163.41
India	-17.55	143.27	203.21
NAC	-22.31	3.46	174.80
WAC	-8.17	15.34	157.48
SAC	5.35	27.71	146.23
Mawson	7.54	29.47	176.03
North China	-74.68	23.99	163.92
Siberia	-16.13	6.76	94.22
Congo	-21.76	132.35	149.98
São Francisco	-20.55	114.54	108.58
Kalahari	5.78	123.79	120.09
Dronning Maud Land	-13.01	117.09	71.71
Rockall	-61.80	64.66	199.42
Amazonia	-28.31	44.66	-156.73
West Africa	-7.85	61.06	-144.89

1470 Ma

Laurentia	-41.88	52.75	173.88
Greenland	-41.56	56.85	186.46
Baltica	-48.36	22.06	169.89
India	-18.55	139.45	168.79
NAC	-9.30	9.38	195.76
WAC	6.95	15.65	175.94
SAC	21.73	24.01	159.63

Mawson	24.22	30.19	187.30
North China	-57.24	33.09	164.56
Siberia	-1.87	2.57	113.73
Congo	-20.83	128.53	120.35
São Francisco	-14.79	106.36	81.70
Kalahari	12.10	126.65	90.71
Dronning Maud Land	-7.24	105.23	42.78
Rockall	-44.65	63.62	190.33
Amazonia	-15.03	50.40	-155.16
West Africa	5.29	66.97	-149.67

1450 Ma

Laurentia	-49.45	47.34	166.33
Greenland	-49.01	50.83	179.54
Baltica	-52.17	11.71	159.27
India	-24.17	142.17	182.54
NAC	-10.69	7.32	177.96
WAC	4.30	16.48	158.32
SAC	16.42	26.24	145.57
Mawson	18.08	31.02	174.34
North China	-62.78	19.96	157.09
Siberia	-3.00	2.25	95.36
Congo	-26.50	134.70	132.06
São Francisco	-22.40	117.04	88.66
Kalahari	-3.26	-47.66	254.99
Dronning Maud Land	14.52	-52.59	306.61
Rockall	-52.53	57.44	185.10
Amazonia	-24.15	46.31	-164.17
West Africa	-5.12	63.80	-153.62

1380 Ma

Laurentia	-49.30	49.97	168.03
Greenland	-48.95	53.43	181.26
Baltica	-53.02	14.45	160.32
India	-22.33	142.65	182.02
NAC	-11.93	8.07	180.47
WAC	3.35	17.02	161.48
SAC	3.35	17.02	161.48
Mawson	8.52	18.37	189.86
North China	-38.51	28.95	127.44
Siberia	-3.86	4.00	97.84
Congo	-24.44	134.35	131.97
São Francisco	-19.98	115.95	89.69
Kalahari	-22.80	-19.79	257.70
Dronning Maud Land	-41.43	-23.88	309.43
Rockall	-52.33	60.31	186.59
Amazonia	-19.63	42.62	-146.16
West Africa	2.30	58.21	-142.29

1270 Ma

Laurentia	-45.58	33.22	147.89
Greenland	-45.06	37.64	160.47
Baltica	-41.66	1.14	147.80
India	-37.45	141.73	176.32
NAC	-10.76	16.93	149.35
WAC	4.24	30.23	136.50

SAC	4.24	30.23	136.50
Mawson	5.78	31.67	166.53
North China	-30.43	48.99	90.41
Siberia	11.06	-8.90	85.16
Congo	-40.05	141.07	124.22
São Francisco	-36.71	129.99	75.14
Kalahari	-26.92	13.49	204.38
Dronning Maud Land	-49.93	12.66	241.22
Rockall	-49.41	42.11	166.77
Amazonia	13.74	37.53	-145.13
West Africa	32.71	53.30	-166.16

1790 Ma in Fig. 5(a-c)

Laurentia	-56.21	45.56	221.94
Greenland	-54.83	47.70	235.53
Fennoscandia	-67.76	3.72	206.77
Sarmatia/Volgo-Uralia	-57.35	-28.40	176.11
Amazonia	-75.57	46.84	120.87
West Africa	-62.41	77.36	161.15
Rockall	-56.32	58.03	241.86

1420 Ma in Fig. 5(d-f)

Laurentia	-39.89	41.09	165.36
Greenland	-39.30	45.53	177.53
Baltica	-42.22	11.08	166.41
Amazonia	-51.59	6.39	91.42
West Africa	-51.89	52.92	116.82
Rockall	-43.03	51.20	182.20